EXAMINING THE IMPACT OF THE ISLAND MASS EFFECT ON CARBONATE CHEMISTRY IN THE NEARSHORE REEF ECOSYSTEM OF THE NORTHWESTERN HAWAIIAN ISLANDS

A THESIS SUBMITTED TO THE GRADUATE DIVISION OF HAWAII PACIFIC UNIVERSITY IN PARTIAL FULFILLMENT OF THE REQUIREMENTS FOR THE DEGREE OF

MASTER OF SCIENCE

IN
MARINE SCIENCE

MAY 2016

By
Crystal T. Henkel

Thesis Committee:
Samuel E. Kahng, Chairperson
Chris D. Winn
Fred T. Mackenzie

EXAMINING THE IMPACT OF THE ISLAND MASS EFFECT ON CARBONATE CHEMISTRY IN THE NEARSHORE REEF ECOSYSTEM OF THE NORTHWESTERN HAWAIIAN ISLANDS

C. T. Henkel

TABLE OF CONTENTS

Acknowledgement

First, I would like to thank my wonderful husband, Rich Henkel, for supporting me throughout my masters. He made this degree possible in every way possible.

Thank you to my advisor Dr. Sam Kahng, along with my advisory committee Dr. Chris Winn and Dr. Fred Mackenzie for their patience, feedback, and intellectual support.

Thanks to the Papahānaumokuākea Marine National Monument, NOAA, and the R/V Searcher crew for making a once in a lifetime research cruise to French Frigate Shoals possible. Thank you for the research funds which made this work possible provided by NOAA's Office of National Marine Sanctuaries through the Papahānaumokuākea Marine National Monument.

Thank you to the Hawaii Ocean Time-series program coordinators for an amazing opportunity to join them on two research cruises to see how the data I used was actually measured!

Thank you to Melissa Eyre for always caring, listening, and trying to help whenever possible. Thanks to all the graduate students at HPU, especially Roman Battisti and Meagan Putts for their feedback on this work and the stimulating (mostly) scientific discussions in and out of the classroom. Thanks to Luke Snedaker, Austin Tubbs, and Estefina Escalante for being awesome laboratory technicians, you definitely made my life easier.

A special thanks to all of my Hawaii friends, Randall Scarborough, Emma Forbes, Gabriella Runko, Shane Krackenberger, Sarah Leicht, Dan Severino, and Elise Kohli that have reminded me to take the time to have fun every once in awhile. You kept Rich and I sane throughout this process!

Thank you to my family, Cindi Heydet, Greg Heydet, Jen Spitler, and Mike Spitler, and long time friends for providing me nothing but love and support.

Finally, another huge thank you to my amazing husband Rich Henkel! Thank you for your patience, encouragement, and support while I worked towards my masters.

Abstract

The rising atmospheric and hence surface ocean pCO_2 is forecasted to alter rates of calcification and dissolution of coral reef ecosystems globally. Much of what is known about marine CO_2-carbonic acid system chemistry is based on either analysis of open ocean waters or intensive characterizations of the marine carbon chemistry of specific reefs on a small spatial scale. However, analysis of coastal ocean reef systems is lacking. In particular, whether the accretion rate of low-lying coral atolls and islets can outpace the projected sea level rise is unknown. Four years of carbon system data were analyzed to characterize the net calcification of the reef ecosystem of the Northwestern Hawaiian Islands in the Papahānaumokuākea Marine National Monument. Discrete bottle samples (n=1073) were collected via CTD hydrocasts (n=275) to measure alkalinity from nearshore transects along the 1,500-mile archipelago. A consistent and significant mean alkalinity deficit between 3.4 and 32.8 μmol/kg (compared to open ocean waters) was detected up to 7.0-23.4 km from emergent land with a significant archipelago gradient. At French Frigate Shoals, the spatial characteristics of the alkalinity deficit, bathymetry, surface currents, and island density proxies were used to calculate net $CaCO_3$ production and carbonate island and atoll platform vertical accretion rates. The results provide vital insight into whether these islands will outpace sea level rise and plate subsidence and will determine the viability of critical nesting and rearing habitat for endangered/threatened monk seal, sea turtle, and seabird species.

Chapter 1: Introduction

1.1 Ocean Acidification

The term ocean acidification originated to describe the increase in uptake of CO_2 by the surface ocean and subsequent reduction in pH due to increasing atmospheric pCO_2 (Gattuso and Hansson 2011). The concentration of greenhouse gases, including CO_2, in the atmosphere and the ocean is on the rise due to burning of fossil fuels, cement production, and deforestation (Sabine et al. 2004; Kleypas and Langdon 2006). Drilling at the Vostok station in East Antarctica has revealed records of the atmospheric composition and climate for the past four glacial-interglacial cycles (Petit et al. 1999). For the 650,000 years prior to the start of the Industrial Revolution the pCO_2 of the atmosphere ranged from 180 to 300 parts per million by volume (ppmv) (Petit et al. 1999; Kleypas and Langdon 2006; Solomon et al. 2007; Gattuso and Hansson 2011). The concentration of CO_2 in the Earth's atmosphere has risen roughly 40% since the start of the Industrial Revolution to more than 400 ppmv (Zeebe and Zachos 2013); (National Oceanic and Atmospheric Administration; United States Environmental Protection Agency). To date roughly 25-30% of all anthropogenic carbon dioxide released to the atmosphere has dissolved in the surface waters of the ocean (Sabine et al. 2004; Kleypas et al. 2006; Feely et al. 2009; Andersson and Gledhill 2012; Cyronak et al. 2013; Shamberger et al. 2014). The surface ocean pH is roughly 0.1 units lower today than the pre-industrial level (Solomon et al. 2007). The current rate of ocean acidification is estimated to be 100 times faster than any time in the past one million years and may be unprecedented in Earth's history (Talmage and Gobler 2009).

1.2 Potential Impact of Ocean Acidification

A void exists in analysis and predictions of how the coastal reef ecosystem will react to ocean acidification (OA) with respect to temporal and spatial factors which may impact the ability of calcifiers to adapt quickly enough to survive these changes (Andersson et al. 2007).

Increasing CO_2 in the surface ocean decreases pH and changes the dissolved inorganic carbon species composition in the surface ocean (Zeebe and Wolf-Gladrow 2001; Morse and Arvidson 2002; Cyronak et al. 2013). The rapid increase in atmospheric and surface ocean CO_2 concentrations has the potential to drastically alter the biotic and abiotic metabolic processes that control the nearshore reef ecosystem (Cyronak et al. 2013). Ocean acidification can have inhibitory effects on critical biological functions including marine calcification, reproduction, photosynthesis, and respiration (Gattuso et al. 2011; Cyronak et al. 2013). Corals, crustose corraline algae, halimeda, foraminifera, coccolithophores, bryozoans, mollusks, echinoderms, bivalves (oysters, clams, and mussels), pteropods, and phytoplankton are some of the many marine calcifiers that appear very sensitive to changes in carbonate chemistry (Feely et al. 2004; Guinotte and Fabry 2008; Feely et al. 2009). Potential effects of ocean acidification (OA) on many non-calcifying species, especially higher-trophic level organisms that rely on calcifiers for shelter and nutrition, are largely unknown and can only be theorized (Andersson et al. 2007). Coral reefs are considered the most biologically diverse ecosystem supporting nearly one third of all accepted described marine species on the planet (Veron 2008). The long-term viability of coral reef ecosystems is not understood in a high-CO_2 environment and may impact the estimated one million species that depend on coral reef habitat (Albright et al. 2010).

1.3 Seawater Carbonate Chemistry

Carbon dioxide reacts with the water to form a weak acid that dissociates into the dissolved inorganic carbon constituents (Zeebe and Wolf-Gladrow 2001). The reactivity of CO_2 with seawater slows down the more than 200 day equilibration process as only gaseous CO_2 in the ocean can exchange with the atmosphere (Zeebe and Wolf-Gladrow 2001).

Dissolution of CO_2 in seawater changes the total dissolved inorganic carbon

concentration and the carbon speciation composition. Carbon dioxide readily dissolves in seawater to form the aqueous phase of carbon dioxide (Zeebe and Wolf-Gladrow 2001; Millero 2007).

$$CO_2(gas) \rightarrow CO_2(aq)$$

However, in the current surface seawater conditions less than 0.5% of the aqueous carbon dioxide formed stays in this carbon species (Zeebe and Wolf-Gladrow 2001). Most of the aqueous carbon dioxide is immediately hydrated to form carbonic acid (H_2CO_3), a weak acid (Zeebe and Wolf-Gladrow 2001; Gattuso and Hansson 2011).

$$CO_2 + H_2O \rightarrow H_2CO_3$$

The two electrically neutral forms of CO_2 in seawater, CO_2(aq) and H_2CO_3, are not chemically separable and together the concentration accounts for less than one percent (Zeebe and Wolf-Gladrow 2001; Emerson and Hedges 2008). The majority of the carbonic acid that forms instantly dissociates to bicarbonate ions (HCO_3^-) and carbonate ions (CO_3^{2-}) in two acid base reactions (Zeebe et al 2001).

$$H_2CO_3 \leftrightarrow H^+ + HCO_3^-$$

$$HCO_3^- \leftrightarrow H^+ + CO_3^{2-}$$

These reactions simplify to a single reaction that better describes the carbonate system reaction to input of CO_2 in seawater:

$$CO_2 + H_2O + CO_3^{2-} \rightarrow 2HCO_3^-$$

The percent composition of the chemical species that make up the carbonate system are controlled by the pH, salinity, temperature, and total Dissolved Inorganic Carbon (DIC) of the seawater (Zeebe and Wolf-Gladrow 2001).

1.4 Ocean Acidification Terminology & Measurement Parameters

There are four main terms, total alkalinity (TA), dissolved inorganic carbon (DIC), pCO_2, and pH, used to define the ocean carbonate system (Zeebe et al. 2001). The knowledge of any two of the four carbonate system parameters allows you to calculate the remaining carbonate chemistry parameters of the seawater system (Zeebe et al. 2001).

The pH scale is a logarithmic measure of the hydrogen ion concentration in solution ($pH = -\log[H^+]$). pH can be reported using several different scales, but the scales do not relate with a simple offset so conversion from one to another is difficult. The total scale is typically utilized in oceanography experiments and will be for this work.

Dissolved inorganic carbon (DIC) measures the concentration of the main dissolved forms of inorganic carbon in seawater: aqueous carbon dioxide ($CO_{2(aq)}$), carbonic acid (H_2CO_3), bicarbonate (HCO_3^-), and carbonate ion (CO_3^{2-}) (Zeebe et al 2001).

$$DIC = C_T = [H_2CO_3] + [CO_2(aq)] + [HCO_3^-] + [CO_3^{2-}]$$

The chemical speciation of carbon in seawater responds to changes in total DIC, temperature, salinity, and pressure (Zeebe and Wolf-Gladrow 2001).

DIC is a conservative property, so changes in temperature, pressure, and salinity will not change its total value (Zeebe and Wolf-Gladrow 2001). However, the speciation of the carbon species that make up DIC will vary with temperature, pressure, and salinity. An increase in temperature drives seawater away from carbonate ions towards carbon dioxide (Zeebe and Wolf-Gladrow 2001). An increase in salinity moves the carbon species in the same manner, away from carbonate ions towards carbon dioxide (Zeebe and Wolf-Gladrow 2001). An increase in pressure will move the carbon species away from carbon dioxide increasing carbonate ion concentration (Zeebe and Wolf-Gladrow 2001).

Carbon dioxide partial pressure, pCO_2, is the partial pressure of CO_2 in the gas phase that

is in equilibrium with seawater for a given region (Zeebe et al. 2001). The difference between the partial pressure in the ocean and atmosphere determines the net air-sea gas CO_2 flux rate and direction (Zeebe and Wolf-Gladrow 2001; Takahashi et al. 2002; Fagan and Mackenzie 2007). The atmospheric and oceanic pCO_2 are in constant flux, moving towards equilibrium despite perpetually changing carbon inputs and outputs to either system. The solubility of carbon dioxide in the surface waters of the ocean is largely based on sea surface temperature (SST) and wind speed (Zeebe and Ridgwell 2011). Greater wind speed increases the rate of air-sea gas exchange (Wanninkhof 1992; Feely et al. 1999; Fagan and Mackenzie 2007).

Total alkalinity (TA) is a measure of the charge balance of the conservative ions in seawater and can be described as the capacity of a solution to neutralize hydrogen ions (Chisholm and Gattuso 1991; Zeebe and Wolf-Gladrow 2001). The buffer capacity and the alkaline properties of seawater are mainly attributed to the dissolved carbonate species so a change in total alkalinity is nearly equivalent to the change in carbon alkalinity (~95.6%) (Zeebe and Wolf-Gladrow 2001; Sarmiento and Gruber 2006).

$$TA = [HCO_3^-] + 2[CO_3^{2-}] + [B(OH)_4^-] + [OH^-] + [H^+] + minor\ components$$

The charge balance, and therefore the total alkalinity, is not directly affected by dissolution of CO_2 into seawater from the atmosphere. Alkalinity is affected by metabolic processes, but not by air-sea gas exchange (Sarmiento and Gruber, 2006). Alkalinity is a conservative property, so changes in temperature and pressure will not change its total value (Zeebe and Wolf-Gladrow 2001).

Several components of salinity impact the TA and DIC values measured therefore TA and DIC are normalized to remove its effects. Normalized TA and DIC will primarily be analyzed in this study to account for the vertical salinity structure of the water column (C. L. Sabine 1995). Additionally, normalizing TA and DIC allows for a comparison of data sets across seasons by

eliminating some of the effects of temperature, precipitation, and evaporation (C. L. Sabine 1995). The changes observed in normalized TA are attributed to metabolic chemical changes or variations in vertical mixing (C. L. Sabine 1995). The changes observed in normalized DIC are attributed to metabolic chemical changes, variations in vertical mixing, or CO_2 gas solubility changes with temperature (C. L. Sabine 1995).

1.5 Nearshore Metabolic Processes

Four main metabolic processes impact the carbonate chemistry of nearshore reef ecosystems: photosynthesis, respiration, calcification, and dissolution (Zeebe and Wolf-Gladrow 2001; Erez et al. 2011). Metabolic processes in the ocean cause changes in the carbonate chemistry system. The carbonate chemistry system is dynamic; the system reacts to different inputs and outputs to the carbonate system with changes in pH, total alkalinity, pCO_2, and dissolved inorganic carbon (Erez et al. 2011).

Phytoplankton and other photosynthetic organisms chemically change carbon dioxide and water into oxygen and carbohydrates (sugars). Phytoplankton and other marine species consume organic matter and oxygen for energy which they respire as carbon dioxide and water vapor.

$$Photosynthesis \rightarrow \qquad\qquad \leftarrow Respiration$$

$$106CO_2 + 122H_2O + 16HNO_3 + H_3PO_4 + light\ energy$$

$$\rightarrow (CH_2O)_{106}(NH_3)_{16}H_3PO_4 + 138O_2$$

Photosynthesis decreases nDIC and pCO_2 and increases pH and nTA slightly (Erez et al. 2011; Gattuso and Hansson 2011; Jokiel et al. 2014). Respiration increases nDIC and pCO_2 and decreases pH and nTA slightly (Erez et al. 2011; Gattuso and Hansson 2011; Jokiel et al. 2014). The change in DIC drives the change in pH associated with photosynthesis and respiration. A reduction in the total DIC by photosynthesis raises pH while an increase in the total DIC from respiration decreases pH (Zeebe and Wolf-Gladrow 2001). The change in DIC from

photosynthesis and respiration does not change the total alkalinity, but the uptake of one mole of ammonium ($NH4^+$) or nitrate ($NO3^-$) during photosynthesis slightly increases or decreases alkalinity, respectively (Zeebe and Wolf-Gladrow 2001). Respiration or remineralization releases one mole of nitrate which will decrease alkalinity by one mole (Zeebe and Wolf-Gladrow 2001).

Calcification is the process of chemically reducing calcium and bicarbonate or carbonate ions to form the solid mineral $CaCO_3$ (Emerson and Hedges 2008; Gehlen et al. 2011; Andersson and Gledhill 2012). Calcification is thermodynamically favorable in subtropical surface seawater but does not typically spontaneously occur. Instead calcification is primarily biologically mediated by marine calcifiers for growth (Andersson and Gledhill 2012). Dissolution breaks down solid calcium carbonate to its ionic components, calcium and carbonate ions.

$$Calcification, 1:\ Ca^{2+} + 2HCO_3{}^- \rightarrow CaCO_3(s) + H_2O + CO_2$$

$$Calcification, 2:\ Ca^{2+} + CO_3{}^{2-} \rightarrow CaCO_3(s)$$

$$Dissolution:\ CaCO_3(s) \rightarrow Ca^{2+} + CO_3{}^-$$

Calcification decreases nDIC, nTA, and pH and increases pCO_2 locally (Erez et al. 2011; Gattuso and Hansson 2011; Jokiel et al. 2014). Dissolution increases nDIC, nTA, and pH and decreases pCO_2 locally (Erez et al. 2011; Gattuso and Hansson 2011; Jokiel et al. 2014). Calcification can impact pH in two ways: the immediate microenvironment and the long term sequestration of carbon. As calcification of $CaCO_3$ is taking place bicarbonate is being consumed and carbon dioxide is released. Locally an acidic microenvironment is created due to a higher CO_2 level (Zeebe and Wolf-Gladrow 2001). However, calcification sequesters carbon in rock form as $CaCO_3$ removes it from the DIC pool. In a well-mixed environment, calcification lowers DIC which increases pH or makes the environment more basic. Dissolution of $CaCO_3$ will increase pH by driving the system to a higher DIC concentration (Zeebe and Wolf-Gladrow

2001). Calcification of $CaCO_3$ will reduce DIC by removing a carbon molecule from the seawater system (Zeebe and Wolf-Gladrow 2001). Dissolution of $CaCO_3$ will increase DIC by adding a carbon molecule to the seawater system (Zeebe and Wolf-Gladrow 2001).

1.6 Carbon Chemistry Balance in the Surface Ocean

The carbon chemistry balance in the nearshore surface ocean is primarily driven by inorganic and organic reef metabolism. The balance of inorganic (calcification and dissolution) and organic (photosynthesis and respiration) metabolic processes produces a net signal in the nearshore seawater that differs from open ocean values (Zeebe and Wolf-Gladrow 2001; Wolf-Gladrow et al. 2007; Erez et al. 2011). In a coral-dominated, balanced autotrophy and heterotrophy system, the carbon being removed via calcification presents itself as an alkalinity deficit.

Air-sea gas exchange and anaerobic diagenesis in sediments also modify the carbon chemistry in the nearshore surface seawater. Air-sea gas exchange controls the rate of invasion or release of CO_2 between the overlying air and surface seawater (Takahashi et al. 2002). Anaerobic diagenesis and nutrient transformation in sediments in shallow water sediments contributes to total alkalinity (Murillo et al. 2014). The sediments of the nearshore environment may provide a daily net source of alkalinity to the water column (Cyronak et al. 2013). The production of CO_2 from respiration can promote dissolution of the carbonate sediments (Cyronak et al. 2013). The rate of carbonate sediment dissolution is determined by the chemistry of the overlying water, residence time of water, advection rate, sediment composition, and biological activity (Cyronak et al. 2013).

1.7 Island Mass Effect

The island mass effect describes a nearshore region of high productivity compared to the

surrounding open ocean waters; the island mass effect is seen in the waters surrounding the Hawaiian Islands (Doty and Oguri 1956; Heywood et al. 1990). Nearly 30% of all global marine primary productivity occurs in coastal waters (Andersson and Mackenzie 2004). The average carbonate production in the open ocean is much less productive than in the nearshore waters of the Hawaiian Islands; the difference measured is an order of magnitude. The average carbonate production of the Hawaiian Archipelago is approximately 3.9×10^{12} grams $CaCO_3$ per year compared to the global open ocean average of approximately 4.9×10^{11} grams $CaCO_3$ per year (Sabine and Mackenzie 1995). Increased primary production and calcification in coastal waters may impact carbonate chemistry a great distance offshore (Sabine and Mackenzie 1995). The flow disturbance in the wake of the NWHI archipelago can create a phytoplankton bloom during the spring and summer months which can be observed via satellite as an increase in chlorophyll content. Enhanced chlorophyll content is measured in the nearshore environment which decreases moving out radially from the island (Gove et al. 2013). The increased vertical mixing surrounding the island mass can enhance the surface water productivity which can stimulate greater biological carbon dioxide uptake which will increase the flux of CO_2 into the ocean (Caldeira and Wickett 2003; Rudnick et al. 2003).

A 1995 study by Sabine and Mackenzie indicated the Northwestern Hawaiian Islands may have a ‘halo’ of elevated alkalinity around the NWHI banks. Sabine and Mackenzie proposed the ‘halo’ was a result of bank-derived carbonate particle dissolution in the water column from the islands (Sabine and Mackenzie 1995). Presence of the halo implies the islands may have a localized buffering effect as pH increases in the open ocean (Sabine and Mackenzie 1995).

1.7 North Pacific Subtropical Gyre Open Ocean Data Collection

Over the last two decades, several large-scale programs have been established to collect water chemistry data to track the changing ocean environment; two of which can be used as an open ocean proxy for the NPSG. The Hawaii Ocean Time-Series (HOT) was established in 1988 and has helped define the water chemistry characteristics of the North Pacific Subtropical Gyre (Karl 1999). Since its inception the HOT program has been studying the rates and pathways of carbon and energy flow, the spatial and temporal scales of variability, the coupling of ocean physics and biogeochemical processes, and changes in the microbial community structure and nutrient cycling in response to large scale ocean-atmosphere interactions. The HOT ALOHA (A Long-Term Oligotrophic Habitat Assessment) site is 100 km north of the island of Oahu. Data from the HOT program has measured a decrease in pH of 0.02 units per decade indicating that the open ocean waters surrounding the Hawaiian Islands are a net sink for CO_2 (Dore et al. 2003; Dore et al. 2009). Data from the HOT ALOHA site provides insight into seasonal and temporal changes in the open waters surrounding the Hawaiian Archipelago. The World Ocean Circulation Experiment (WOCE) was established to determine the role of the ocean in the Earth's climate. Field samples were gathered that produced a comprehensive data set that covered the entire ocean, all seasons, and set measurement standards globally so comparison of data from different countries and regions is more accurate. The vertical portion of WOCE lines 14 and 16 run to the west and east of the Hawaiian archipelago, respectively (Figure 1). Data from the WOCE lines 14 and 16 provides data on the latitudinal and longitudinal changes in the open ocean and may provide insight into the changes along the Hawaiian Archipelago.

1.9 Alkalinity Anomaly Technique

The alkalinity anomaly technique was developed to calculate an average gross calcification rate using water chemistry measurements of total alkalinity (TA) and dissolved inorganic carbon

(DIC) of samples collected directly above a coral reef ecosystem (Chisholm and Gattuso 1991; Shamberger et al. 2011; Lantz et al. 2013).

Quantifying the net metabolic signal of a coral reef ecosystem using the alkalinity anomaly technique has proven to be much less invasive and time intensive than other short-term monitoring techniques (Smith and Kinsey 1978; Chisholm and Gattuso 1991). The technique is based on the principal that total alkalinity of surface seawater is primarily impacted by precipitation of $CaCO_3$(s) and is not affected appreciably by photosynthesis or respiration (Smith and Kinsey 1978; Chisholm and Gattuso 1991). The foundation of the assumption is that the ecosystem is balanced between net autotrophy and net heterotrophy, which is true for most seawater systems over long time periods but may be less valid over short time periods (Chisholm and Gattuso 1991). Previous work has indicated that the alkalinity anomaly technique does not require correction for changes in concentrations of non-carbonate ions when measuring changes in total alkalinity (Chisholm and Gattuso 1991). The assumption is made that the change in non-conservative non-inorganic carbon species from calcification and dissolution have a negligible impact, less than five percent, on total alkalinity (Chisholm and Gattuso 1991). The alkalinity anomaly technique has one distinct advantage over other short-term calcification rate estimation methods. The alkalinity anomaly technique uses the change in carbonate ion concentration to calculate calcification rate not calcium ion concentration so calcification that occurs as $MgCO_3$ is also be captured in the estimation (Smith and Kinsey 1978; Chisholm and Gattuso 1991). This distinction in especially important in regions with high Mg^{2+} concentrations like the Hawaiian archipelago (Andersson et al. 2005).

1.10 Seawater Residence Time

The residence time of a seawater parcel in a given region can have a dramatic impact on the strength of the signal that can be observed for a shallow seawater ecosystem. Residence time

is an approximation of the average amount of time a water parcel will remain in the ecosystem. Residence time is determined by hydrodynamic forcing and wave and wind speed and direction (Falter et al. 2013). The greater the wave and wind forcing the faster water will move over the reef ecosystem and the shorter the residence time (Falter et al. 2013). Residence time controls the magnitude of change to a water parcel by a biotic or abiotic process (Falter et al. 2013). A longer residence time in a region generally equates with a larger measured metabolic signal (Suzuki and Kawahata 2002; McMahon et al. 2013).

The Hybrid Coordinate Ocean Model (HYCOM) is a mixture of SADCP, buoy, and satellite but the data presented was screened to ensure it accurately depicts the mean surface current rate and direction (NOAA 2015). HYCOM surface currents are believed to be the most accurate approximation of the 'flushing rate' for the NWHIs at this time.

1.11 Island Density

Reference values for bulk island density were scanned from the literature available. Coral density increases with latitude along the NWHI archipelago (Grigg 1981). Average densities for the dominant Hawaiian coral species, *Porites lobata*, measured by X-ray scan range from 1.2 mg/mm^3 at Nihoa and French Frigate Shoals to 1.9 mg/mm^3 at Pearl & Hermes Atoll and Midway Atoll (Grigg 1982). Coral cores collected at roughly the same latitude as FFS in the Pacific Ocean at Ishigaki Island correspond to the values reported for FFS. The skeletal density values ranged from 1.45 to 1.70 +/- 0.02 g/cm^3 (Sowa et al. 2013). Coralline algae cements sediment on the island platform which has a mean bulk density in Barbados of 1.56 mg/mm^3 (Stearn et al. 1977; Harney and Fletcher III 2003). Sand is another major component of a coral island. The density of sand on Oahu was measured at 2.72 mg/mm^3 (Smith and Cheung 2002). The bulk density of sand sediment will be substantially lower due to the packing factor. An

estimate of the packing factor for SiO_2 is 0.63, silica sand is not prevalent in Hawaii, but the density of silica sand is similar to that reported on Oahu beaches around 2.65 mg/mm^3 (Hardisty 1990).

There are several estimations of the dry weight percent of organic matter in stony, warm water corals, but the estimates depend heavily on protocol (Muscatine et al. 2004). Historically the percent weight organic matter of the total skeleton have been reported as a small amount, generally less than 0.1% (Ingalls et al. 2003; Watanabe et al. 2003; Muscatine et al. 2004).

1.12 Reef Accretion

Vertical reef accretion in the NWHI reef ecosystems has enabled the coral islands to stay subaerial despite rising sea level, plate subsidence, dissolution, and erosion (Grigg 1982). Since 1974 the average relative sea level at French Frigate Shoals has risen at approximately 0.61 mm/yr (Church et al. 2006; (PSMSL) 2016). However according to the latest IPCC report, for the remainder of the 21st century the sea level rise rate is projected between 3.0 and 9.5 mm/yr, an order of magnitude greater than the previous century (Church et al. 2006; Rooney et al. 2008; Szabados 2008; Edenhofer et al. 2014; (PSMSL) 2016).

In the past 19,000 years the sea level around the Hawaiian Islands has risen an estimated 120 m (Rooney et al. 2008). Geological studies have reported that more than the upper 100 m of the NWHIs are limestone, not the basalt originally deposited from the islands' volcanic origins (Gross et al. 1969; Ladd et al. 1970; Rooney et al. 2008). The NWHIs were formed via a hot spot in the Earth's mantle, as the NWHIs move away the crust cools and subsides at a rate of roughly 0.02 to 0.03 mm/yr (Grigg and Epp 1989; Stein and Stein 1992; Rooney et al. 2008). Over time, erosion and redistribution of mass via mechanical processes and biogenic dissolution estimated between 0.05 to 9.11 mm/yr have decreased the NWHIs' platform size (Grigg and Epp 1989).

Carbonate sediments primarily produced by bioerosion are not generally exported from the island shelf by the normal tidal current but are primarily flushed from the reef by major storms (Hine et al. 1981; Sadd 1984; Hubbard et al. 1990; Hubbard 1992). Between 18 and 27% of total carbonate production on a reef is estimated to be exported off the island shelf (Land 1979; Sadd 1984; Hubbard et al. 1990; Hubbard 1992; Harney and Fletcher III 2003).

1.13 NWHI Setting

The Northwestern Hawaiian Islands present an interesting region of the global ocean to study and the NWHIs span over 1100 miles and 5.25 degrees latitude. The NWHI have warm surface waters, the average annual surface water temperatures for the archipelago range between 23 and 27°C throughout the year (Juvik et al. 1998; Karl 1999; Desch et al. 2009)). The surface mix layer depth in the NWHI varies seasonably between 40 and 100 m (Karl 1999).

The Hawaiian Islands are the exposed peaks of a great undersea mountain range formed from volcanic activity over a hotspot in the Earth's mantle. The Hawaiian Islands therefore comprised primarily of igneous basalt (Gove et al. 2013). All of the NWHI are slowly sinking and have experienced significant erosion of the basalt from which they were originally formed. Calcium carbonate from coral reef formation has taken the place of the basalt; the upward growth of the coral reef is the only thing keeping many atolls and islets at sea level (Grigg et al. 2008b). Laysan and Lisianski are coral islands and Pearl and Hermes, Midway, and Kure are coral atolls. Kure atoll is the farthest atoll northeast in the Hawaiian Island chain and the coral growth is believed to match the negative losses caused by bioerosion, mechanical erosion, and subsidence (Hubbard 1997; Grigg et al. 2008b).

The solubility characteristics and predominance of magnesium calcite carbonate crystals in the Northwestern Hawaiian Islands makes it a unique place to study. Calcareous organisms

that produce very soluble magnesium calcite and aragonite phases are abundant throughout the Hawaiian archipelago (Sabine and Mackenzie 1995). The abundance of magnesian calcites increase with depth and northwest direction along the Hawaiian archipelago (Sabine and Mackenzie 1995). The sediment on the Northwestern Hawaiian Island banks are dominated by magnesian calcites which are more soluble than calcium carbonate compounds that dominate most other areas where coral reef proliferates (Sabine and Mackenzie 1995; Andersson et al. 2007; Andersson and Gledhill 2012).

1.13.a Spatial Gradients

1.13.a.1 Change with Depth

The NWHI vertical profiles closely resemble the Hawaii Ocean Time-series (HOT) program station ALOHA data except the surface mix layer closest to the island. With increasing depth from the surface to 1000 m depth at station ALOHA and along the NWHI, nTA and nDIC increase with increasing depth (SOEST 2014; Thompson et al. 2014). pH decreases with increasing depth from the surface to 800 m depth where pH experiences a minimum and then slowly increases with increasing depth (SOEST 2014). pCO_2 follows a similar pattern, increasing with depth as nDIC increases and pH decreases to a depth around 800 m and then increases slightly to a depth of 1000 m (SOEST 2014). The main areas of deviation observed in the NWHI data set from HOT station ALOHA are within the first roughly 100 dbar, therefore the surface ocean will be the primary research focus.

The carbonate measurements in the NWHIs' surface mix layer indicates a net reef ecosystem metabolic signal when compared to the open ocean. The surface mix layer captures the majority of the benthic community production signal in the NWHIs. The surface mix layer is the upper oceanic layer in which turbulence homogenizes the seawater resulting in uniform

temperature, salinity, and density (Brainerd and Gregg 1995). Much of the coral reef ecosystem surrounding the islands and atolls exists in a shallow ecosystem where the total bottom depth is less than the surface mix layer depth (Kleypas and Langdon 2006; Kleypas et al. 2011; Falter et al. 2013). The surface mix layer is generally defined as the upper water column to a depth where the sigma theta is 0.025 kg/m^3 greater than the surface value (SOEST 2014). However, with increased distance from the island center the bottom depth generally increases and eventually the bottom depth is below the surface mix layer. There is little exchange or mixing between the surface mix layer and the subthermocline layer below except in areas of rough interior topography (Wunsch and Ferrari 2004). Additionally, the greatest rates of calcification for corals and reefs occur at depths between 5 to 10 m and decline rapidly with increasing depth (Grigg and Epp 1989). The alkalinity deficit will primarily represent calcification occurring in the surface mix layer but will also include a small contribution of calcification measured as an alkalinity deficit in the upper subthermocline (Figure 2).

1.13.a.2 Distance from Island

The island mass effect is strongest close to the island and is diluted by horizontal and vertical mixing moving out from the island (Thompson et al. 2014). A general trend of decreased pCO_2 was observed moving out radially from the NWHI archipelago with elevated pCO_2 above the open ocean values observed up to 50 km from the nearest reef (Kealoha et al. 2015). A general trend of increasing nTA and decreasing pH were observed moving out from the NWHIs (Thompson et al. 2014). With greater distance from the island, the carbonate parameter values more closely resemble the open ocean (Sabine and Mackenzie 1995; Thompson et al. 2014; Kealoha et al. 2015).

High chlorophyll-a concentration in the nearshore waters of Pearl and Hermes Atoll

indicates that the production rate close to the island dwarfs that of the surrounding oligotrophic waters (Gove et al. 2013). The nearshore community in the NWHI indicated a sharp decline in chlorophyll-a concentration with distance from Pearl and Hermes Atoll from the 30 m contour line to roughly 10 km out from the atoll (Gove et al. 2013). The biomass of primary producers in the nearshore waters surrounding Pearl and Hermes Atoll were on average an order of magnitude higher than the values measured greater than 10 km from the atoll (Gove et al. 2013).

1.13.a.3 Symmetry

Symmetry of the island mass effect is not well studied in the NWHIs with respect to the carbonate parameters. Chlorophyll-a concentration can be a reference for primary producer biomass and no difference was observed for the chlorophyll-a concentration based on the direction measured in a 10 yr study at Pearl and Hermes Atoll (Gove et al. 2013). However, the prevailing summertime surface current across the NWHIs is due to the Northeast Tradewinds which generate a current moving from the east-northeast to the west-southwest (Heywood et al. 1990; Signorini et al. 1999; Fletcher et al. 2008).

1.13.a.4 Latitudinal Gradient

Along the NWHI, with increasing latitude a slight trend of increasing pCO_2 and a trend of decreasing nTA, nDIC, and pH is observed (Kealoha et al. 2015). A trend of decreasing pH with increasing latitude between 20 and 30 °N has been identified in the open ocean sampling of WOCE lines P14 and P16 in 2007 and 2006, respectively (Kealoha et al. 2015). A trend of decreasing aragonite saturation state with increasing latitude was also observed during the 2006 and 2007 WOCE studies (Kealoha et al. 2015). A decreasing saturation state was measured in the nearshore ecosystem moving northwest up the NWHI archipelago (Grigg et al. 1981).

Most water quality features such as salinity, oxygen concentration, turbidity, nitrate

concentration, particulate carbon, chlorophyll a, and biological activity in the pelagic zone are relatively constant throughout the NWHI Archipelago (Grigg et al. 2008b). Coral and algal growth rates are specific to the species, environment, global location, and season (Andersson and Gledhill 2012). For hermatypic, or stony reef building, corals, light may be the most important parameter controlling calcification and growth rates (Hubbard 1997; Andersson and Gledhill 2012). However, temperature, food, nutrients, hydrographic regime, and seawater carbonate chemistry are also critical controls of calcification and growth rates for hermatypic corals (Andersson and Gledhill 2012). Coral calcification rate decreases with increasing latitude along the NWHI chain (Grigg 1981). Coral abundance surrounding a land mass is largely dependent on the wave energy it experiences. The average annual wave energy increases moving northwest along the Hawaiian archipelago (Gove et al. 2013)). Within the Hawaiian archipelago there is significant variability of coral abundance and species diversity. Both coral abundance and species diversity peak at French Frigate Shoals and Maro Reef (Grigg et al. 2008b). Both habitats are large open atolls which minimize disturbance and shelter the corals from wave energy which provides optimal conditions for coral reef accretion (Hubbard 1997). The small islets Necker and Nihoa are further southeast but the islets are openly exposed to severe wave events seasonally. One third fewer species are found at the southeastern islets, Necker and Nihoa, compared to French Frigate Shoals and Maro Reef (Grigg et al. 2008b).

Large swells that come with winter storms limit coral growth and cover on the northwest portions of the NWHI. On average there are 12 to 18 large swell events every winter which produce waves between 10 to 12 m in vertical height (Grigg et al. 2008b). Sine waves of 10 to 12 m breaks at depths similar to the vertical height limiting coral growth in the shallow waters of the north and western sides of the island, islets, and atolls in the winter months (Caldwell 2005)

(Grigg et al. 2008b). Coral cover is lower than the average of 20 percent coral cover throughout the archipelago on the north and west portion of the island, islets, and atolls which have around five to 10 percent coral cover (Grigg et al. 2008b; Milliman et al. 2012).

Seawater temperatures in some portions of the NWHI are close to the lower temperature limit of many shallow, warm water corals which can negatively impact coral abundance (Grigg 1981; Sheppard et al. 2009; Dubinsky and Falkowski 2011). Seawater temperature varies substantially with latitude and depth and affects coral reef growth. Water temperature is one of the major oceanographic features controlling the distribution and abundance of coral cover in the NWHI. Strong stratification of the water column in the upper regions of the NWHI may restrict shallow, warm water coral reef growth to 20 m or less because the corals cannot survive in the cold temperatures that exist below the shallow thermocline (Sheppard et al. 2009). Midway and Kure Atoll are at the northwestern most section of the Hawaiian archipelago and experience much lower winter water temperatures and lower average annual solar radiation (Grigg et al. 2008b). One third fewer species are found at Midway and Kure Atoll compared to French Frigate Shoals and Maro Reef (Grigg et al. 2008b).

The surface water temperatures and the chlorophyll content in the northwestern portion of the NWHI archipelago are affected by the Transition Zone Chlorophyll Front (TZCF). The TZCF is located between the subtropical and subpolar gyres and generally stays between 45 and 30°N migrating farther south in the winter. The TZCF increases the nutrient availability and productivity in the northwestern most islands in the Hawaiian archipelago during some winter months but the southern-most latitude of the TZCF varies across years (Polovina et al. 2001).

A general trend of increasing seawater residence time is observed moving northwest along the NWHI archipelago driven by the change in topography of more atolls further northwest and

decreasing Northeast Tradewinds (Falter et al. 2013; Kealoha et al. 2015). The prevailing Northeast Tradewinds more consistently strong in the spring and summer months and are relatively consistent interannually with the exception of ENSO (El Nino Southern Oscillation) years (Juvik et al. 1998; Desch et al. 2009). Historic analysis of the surface current in the NWHIs indicate it is highly variable in both speed and direction but the surface currents predominantly flow from the east-northeast to the west-southwest direction (Firing and Brainard 2006; Desch et al. 2009). The prevailing Northeast Trades are responsible for the surface current in the summertime and the resultant surface current appears to decrease in intensity with latitude (Firing and Brainard 2006; Fletcher et al. 2008).

On average the sea surface temperature (SST) and irradiance level decrease moving northwest up the NWHI archipelago (Desch et al. 2009; Gove et al. 2013). In general the summer sea surface temperatures vary very little along the archipelago in contrast to the SST gradient observed along the NWHI archipelago in the winter (Desch et al. 2009). At the southern portion of the NWHI archipelago the annual SST range is roughly four degrees Celsius whereas the annual SST range is rougly 10 °C at the northern portion of the NWHI archipelago (Desch et al. 2009). The difference in SST along the NWHI archipelago impacts the gas solubility; in the winter a greater gradient in the CO_2 solubility in the surface waters develops along the NWHIs (Drupp et al. 2013; Garbe et al. 2014).

In the latitudinal range of the NWHI, roughly 19°N to 29°N, a sharp drop in the abundance of shallow, warm water corals with increasing latitude is reported (Schlanger and Konishi 1975; Grigg 1981). Calcification rates of individual corals and coral reef accretion declines as latitude increases from the island of Hawaii to Kure Atoll (Grigg 1981). However, the change in ecosystem calcification rates with latitude has not been fully investigated. The decline in individual coral

calcification rates and coral reef accretion does not necessarily lead to a decrease in calcification for the shallow water community; other calcareous organisms may compensate for the decrease in coral calcification at mid-latitudes (Grigg 1981). Percent coral cover generally decreases with latitude with a few exceptions, French Frigate Shoals and Maro Reef both have high coral cover for their high latitude (Grigg 1981).

1.13.b Temporal Variability

1.13.b.1 Diel

The diel cycle of the carbonate system is the net result of the balance between calcification, photosynthesis, respiration, dissolution and air-sea gas exchange in a reef ecosystem (Suzuki et al. 1995; Bates et al. 2010; Shamberger et al. 2011; Drupp et al. 2013; Andersson et al. 2014). Many nearshore ecosystems are net photosynthesis and net calcifying when the sun is overhead, but transition to net respiring and net dissolution after sunset (Bates et al. 2010; Shamberger et al. 2011). At sunrise the pH is the lowest of the day while alkalinity, dissolved inorganic carbon (DIC), and pCO_2 are at the highest value of the day (Suzuki and Kawahata 2002; Lantz et al. 2013; Jokiel et al. 2014). The values of the carbonate parameters at sunrise are driven by reef respiration and increased dissolution which occurs at night. Throughout the day photosynthesis and calcification are driven by the sun's irradiance which increases pH and reduces alkalinity, DIC, and pCO_2. Around sunset the highest daily pH and lowest daily TA, DIC, and pCO_2 are experienced in well-mixed nearshore coral-dominated ecosystems (Suzuki et al. 1995; Shamberger et al. 2011; Lantz et al. 2013; Jokiel et al. 2014). Throughout the daylight hours, nDIC decreases as pH increases which reduces pCO_2 but at the same time calcification is occurring which locally concentrates pCO_2 which results in a greater air-sea CO_2 disequilibrium (Gattuso et al. 1996; Fagan and Mackenzie 2007; Kealoha et al. 2015).

1.13.b.2 Seasonal

Seasonally photosynthesis is highest in spring and summer in the subtropical regions due to greater irradiance intensity, longer length of day, and greater nutrient concentration during spring and summer months (Letelier et al. 2004; Miller and Wheeler 2012). Photosynthesis is lowest in winter for the opposite reasons. Generally the central NPSG is balanced between net autotrophy and net heterotrophy, but at times some nearshore ecosystems can experience net autotrophy or net heterotrophy (Bates et al. 2010). In early summer, macroalgae biomass can quickly build up to its annual maximum and the ecosystem can be net autotrophic (Bates et al. 2010). In late summer, the ecosystem can be net heterotrophic from decreasing macroalgae biomass due to reduced zooxanthellae photosynthetic rates, macroalgae respiration, and remineralization of organic matter (Bates et al. 2010). Biologically-mediated calcification increases with greater irradiance, therefore the rates of calcification follows the same seasonal cycle, highest in spring and summer and lowest in winter (Small and Adey 2001; Bates et al. 2010; Shamberger et al. 2011; Tambutté and Ferrier-Pagès 2013).

Along Lady Elliot Island in the southern Great Barrier Reef region, nTA and nDIC are relatively constant throughout the year with a slight decrease in spring and a dramatic decrease in both measurements in the summer months (Shaw and McNeil 2014). With the effects of temperature removed, the temperature normalized pH and pCO_2 values are relatively constant throughout the year (Shaw and McNeil 2014). Similar results were observed across the reef platform in Bermuda, pH was relatively constant across all seasons, but nTA and nDIC declined substantially in summer and early fall (Yeakel et al. 2015). In subtropical regions, the seasonal difference in sea surface temperature is minimal so the biologically mediated carbon sequestration has a greater driving force than gas solubility changes with temperature in the shallow, nearshore

reef ecosystem (Feely et al. 1999). Summer is the time of greatest carbon uptake due to biologically mediated carbon sequestration despite the warm surface seawater temperatures (Feely et al. 1999). A slight increase in pCO_2 and slight decrease in pH may be observed locally due to increased calcification rates during the summer months (Andersson and Mackenzie 2004).

1.13.b.3 Interannual

Differences in physical forcings drives interannual variability in the values of the carbonate chemistry parameters (Bates et al. 1996; Brix et al. 2004; Falter et al. 2013). From year to year, climate disturbances can impact the winter storm intensity, wind speed and direction, and wave height, speed, and direction which impacts the resulting sea surface temperature, sea surface salinity, air-sea gas exchange, residence time, and mix layer depth for an ecosystem (Brix et al. 2004; Falter et al. 2013). In the surface ocean, a steady increase in nDIC and decrease in pH has been observed at subtropical open ocean sites HOT station ALOHA and BATS due to surface ocean uptake of CO_2(g) (Bates et al. 2014). An increase in nDIC of 1.12 ± 0.04 µmol/kg/y and decrease of 0.0017 ± 0.0001 pH units year are reported for BATS and an increase in nDIC of 1.05 ± 0.05 µmol/kg/y and decrease of 0.0016 ± 0.0001 pH units per year are reported for HOT station ALOHA (Bates et al. 2014). Salinity normalized alkalinity is not impacted by CO_2 input directly so the open ocean surface values have remained relatively stable over the past 25 years (Bates et al. 2014).

CHAPTER 2: ARE NET CALCIFICATION AND CARBONATE ISLAND & ATOLL VERTICAL ACCRETION RATES OF THE NORTHWESTERN HAWAIIAN ISLANDS KEEPING PACE WITH RISING SEA LEVEL?

2.1 Introduction

[MRP1] On a global scale, low-lying reef islands [MRP2]face multiple anthropogenic

threats including accelerated sea level rise, ocean acidification, and warming surface seawater (Hubbard 1997; Hughes et al. 2003; Kennedy et al. 2013; Ford and Kench 2015; Jones et al. 2015; Kench et al. 2015; Spalding and Brown 2015). The reef ecosystem surrounding coral islands provide economic benefit to many countries and critical habitats for a diversity of species (Turner et al. 1996; Wilkinson 1996; Nicholls et al. 2007). Ocean acidification is shifting ocean chemistry outside of its historical range (Andersson et al. 2003; Andersson et al. 2005; Kayanne et al. 2005; Andersson et al. 2015). These chemical changes are predicted to reduce biogenic calcification and promote greater $CaCO_3$ dissolution (Andersson et al. 2003; Andersson et al. 2005; Kayanne et al. 2005; Andersson et al. 2007; Yates et al. 2007; Gattuso and Hansson 2011; Gattuso et al. 2011; Venti et al. 2012; Eyre et al. 2014).

Low-lying islands, islets, and atolls rely on net $CaCO_3$ production and sediment cementation for vertical accretion to remain subaerial (Grigg 1982; Grigg and Epp 1989; Grigg 2006; Kench et al. 2015). The IPCC projections for the rest of the 21st century forecast an accelerated sea level rise which may threaten the continued existence of coral islands and atolls like the Northwestern Hawaiian Islands (NWHI) (http://www.psmsl.org/data/obtaining/) (Church et al. 2004; Church et al. 2006; Church et al. 2013). The low-lying islands of Papahānaumokuākea Marine National Monument (PMNM) in the NWHI serves as critical habitat for endemic, endangered and threatened species like the Hawaiian monk seal, green sea turtle, and several seabirds (Friedlander and DeMartini 2002; Boland and Donohue 2003; Baker et al. 2007; Friedlander et al. 2008). The vertical reef accretion rate is therefore important to the sustainability of these habitats (Yamano et al. 2005; Baker et al. 2007).

Vertical accretion rate derived from net $CaCO_3$ production can project the stability and maintenance of carbonate islands and atolls (Perry et al. 2012; Venti et al. 2012; Kench et al.

2014; Kench et al. 2015; Ford and Kench 2016). There are several ways to quantify net calcification. Geological rate calculations and aerial surveys provide long term net $CaCO_3$ production rates whereas the census-based and hydrochemical approaches provide short term net $CaCO_3$ production rates. Geological rate calculations utilize measurements of the linear extension of annual coral growth bands combined with estimates of areal coverage but, do not represent the carbonate island or atoll as a whole (Grigg 1981) . Aerial surveys quantify changes in the subaerial land mass, but not changes in overall reef structure or the total carbonate island or atoll platform area (Kench et al. 2014; Ford and Kench 2015; Kench et al. 2015; Ford and Kench 2016). The census-based approach surveys an area, recording the benthic cover and assigns a calcification rate to each type of calcifer which is then scaled up using the fraction of the total reef area occupied by each benthic community type (Perry 2010; Perry et al. 2012; Shaw et al. 2016). The calcification rate of the same coral species can be impacted by depth, temperature, solar radiation, and water flow which are difficult to account for properly using the census-based approach (Lantz et al. 2013; Shaw et al. 2016). In addition, the census-based approach is generally coral and coralline algae centric and may miss major contributors like foraminifera or *Halimeda* which may have low calcification rates but cover large areas (Hallock 1981; Rees et al. 2007; Spalding 2012; Shaw et al. 2016). The utility of characterizing a carbonate island or atoll scale ecosystem by extrapolating from a small area is inherently limited when monitoring changes in response to disturbance events (Perry et al. 2013; Shaw et al. 2016). Changes in the total subaerial or reef ecosystem of an island, not an individual reef, will provide the best estimates of $CaCO_3$ production and accretion rates.

The hydrochemical approach can be applied to assess a carbonate island or atoll scale reef ecosystem by measuring the alkalinity deficit in the coastal ocean that is the net result of all

biotic and abiotic process in the ecosystem (Smith and Kinsey 1978; Chisholm and Gattuso 1991; Shamberger et al. 2011; Venti et al. 2012; Lantz et al. 2013; Shaw et al. 2016). [SK3] Understanding the dynamics of the carbonate island or atoll as a whole is important, because an individual reef community can change while the overall amount of reef habitat remains unchanged (Hart and Kench 2007; Venti et al. 2012; Kench et al. 2015). The hydrochemical approach can be applied to the full surface mix layer to approximate the calcification rate for a carbonate island or atoll platform. However the approach is inherently conservative given that water column turbulence and mixing can dilute the chemical signal below detection limits (Chisholm and Gattuso 1991; Shamberger et al. 2011; Lantz et al. 2013). [SK4]

To address the need for carbonate island and atoll scale net $CaCO_3$ production and vertical reef accretion rate estimates, a holistic hydrochemical approach was applied to French Frigate Shoals in the NWHI. Seawater samples collected in the coastal ocean surrounding the reef represent the integrated platform signal (Venti et al. 2012). Subtropical North Pacific Subtropical Gyre (NPSG) open ocean alkalinity is stable over time which provided a basis for comparison to quantify the nearshore calcification signal (Karl and Lukas 1996; McElligott et al. 1998; Millero et al. 1998). Data collected in the coastal ocean were also used to explore carbon system spatial dynamics and gradients along the Hawaiian Archipelago (Andersson and Mackenzie 2004; Andersson et al. 2007; Andersson and Gledhill 2012; Lantz et al. 2013). Discrete bottle samples were collected via conductivity, temperature, and depth (CTD) hydrocasts to measure alkalinity from nearshore transects along the Hawaiian Archipelago. The nearshore measurements from the NWHI were compared to central NPSG open ocean references HOT station ALOHA and portions of WOCE P14 and P16 to analyze the island mass effect (IME), which uncovered a net alkalinity deficit in the surface waters of the NWHI. The spatial extent and variability of the alkalinity deficit

were evaluated. The hydrochemical approach enables calculation of a short-term carbonate island or atoll platform net $CaCO_3$ production and vertical accretion rate using hydrochemical measurements along with bathymetry, surface currents, and island density proxies to address habitat viability in the face of accelerated sea level rise.

2.2 Methods

2.2.a Field Data Collection

Four research cruises to the NWHI were completed during the summer months each year in conjunction with NOAA research efforts and with the support of Papahānaumokuākea Marine National Monument. Two research cruises in the MHIs were completed from late September through November.

Forty-one transects consisting of ~290 conductivity, temperature, and depth (CTD) hydrocasts were completed from 2009 to 2012 in the nearshore waters of the Main and Northwestern Hawaiian Islands to characterize the carbonate chemistry system within the Papahānaumokuākea Marine National Monument (PMNM) (Table 1). Normalized total alkalinity (nTA) was analyzed using abductive reasoning to find spatial trends in the data set. Most of the transects were completed in the lee of the carbonate islands and atolls to optimize the characterization of the island mass effect (Grigg 1983; Desch et al. 2009). Open ocean values from the Hawaii Ocean Time-series (HOT) and World Ocean Circulation Experiment (WOCE) programs were compared to the measurements taken down current of the carbonate islands or atolls to determine the net alkalinity decrease due to reef accretion.

All NWHI transects were completed between 6 pm and 1am with a bearing moving out from the carbonate island or atoll center in the southwest or northeast direction. Transects up to 36 km out began as close to the center of the atoll as feasible. Water samples were collected from the

surface to a depth of 1000 m. Transect locations remained as consistent as possible over the four year sampling period to facilitate temporal comparison.

At a total of 275 stations in the NWHI, CTD hydrocasts were taken in tandem with 1073 discrete bottle samples. A combination of the CTD hydocasts and discrete sample measurement was designed to provide a more complete picture of the carbonate chemistry and oceanographic features surrounding the Hawaiian Islands. The discrete bottle samples were measured for total alkalinity at HPU's Oceanic Institute carbonate chemistry laboratory. Hydrocasts were conducted via CTD rosette with twelve 10 L Niskin bottles.

2.2.b Analytical Measurement

For the CTD hydrocasts, temperature was measured with dual attached SBE 3 temperature probes and reported using the ITS-90 temperature scale with a reported accuracy of +/-0.001°C. Salinity was measured using dual attached aluminum SBE 4 conductivity sensors rated to 6800 m depth with an accuracy of 0.003 PSU.

The discrete bottle samples were measured for total alkalinity using an open cell titration system with an Orion ROSS sure-flow electrode (Gran 1952; Dickson et al. 2007). The bottle sample measurements linked with CTD data provide a more complete spatial and temporal picture of the nearshore ecosystem.

2.2.c Quality Control Procedures

Analytical quality control (QC) for the total alkalinity measurements was maintained with replicate analysis to determine the analytical precision and a duplicate field sample was run at least every 10 samples (Clayton and Byrne 1993; Dickson and Goyet 2005; Dickson et al. 2007). Certified Reference Materials (CRMs) provided by Scripps Institution of Oceanography and Pacific Marine Environmental Laboratory (PMEL) were used to assess accuracy of the total

alkalinity measurements (Dickson and Goyet 2005; Dickson et al. 2007). CRM batch 42, 97, or 122 was measured at the start and end of the nTA measurement period and then at least once every 20 field samples (Table 2).

Cross lab calibration with Bermuda Institute of Ocean Sciences was completed in 2009 providing greater confidence in the absolute total alkalinity measured in the HPU carbonate chemistry laboratory. Additionally, a subset of the discrete samples were sent to Scripps Institution of Oceanography for total alkalinity analysis the same year. Comparison of values measured at the different labs indicated little difference in the mean values (Thompson et al. 2014).

2.2.d Spatial Analysis of the Island Mass Effect Along the Hawaiian Archipelago

To characterize the depth to which the island mass effect extends, vertical depth profiles of the measured nTA collected in the southwest direction of all the carbonate islands and atolls from the surface ocean to 1000 dbar were compared for all the Northwestern Hawaiian Islands (NWHI) with the two central NPSG open ocean references. Sigma theta was used as a proxy for depth so the same water masses were compared along the NWHI archipelago.

The Hawaii Ocean Time-series (HOT) and the World Ocean Circulation Experiment (WOCE) act as a reference for the central NPSG open ocean (Karl and Lukas 1996; Talley et al. 2007). nTA measurements collected between June and September from 2009 through 2012 at HOT station ALOHA were used for this analysis. nTA measurements collected during World Ocean Circulation Experiment (WOCE) lines P14 and P16 (latitudes 19 to 29°N) completed in 2006 and 2007, respectively, were also used in the analysis.

A secondary approach was used to compare mean nTA values of aggregated 0.25 kg/m^3 sigma theta bins from the nearshore NWHI from the surface ocean (~22.625 kg/m^3) to 1000 m deep (~27.375 kg/m^3) with open ocean references. A series of pairwise t tests was used to compare

the mean nTA values for each aggregated sigma theta depth bin to the HOT and WOCE mean values to evaluate statistically significant differences between the nearshore NWHI and either of the open ocean references.

To determine the extent of the IME around each NWHI, the surface mix layer nTA values collected in the southwest transects were compared to the open ocean references (pairwise comparison between each NWHI and each open ocean reference). The IME distance was determined from the latitude and longitude of the center point at each carbonate island or atoll as reported in the 2009 marine biogeographical assessment of the NWHI (Friedlander et al. 2009) with all southwest transect distances calculated as a positive value. The surface mix layer depth (MLD) was calculated for each cast as the depth at which sigma theta is 0.125 kg/m^3 greater than the surface value. The distance at which the nTA values were equivalent to the open ocean reference values with a best fit (highest R^2) line of the surface mix layer measurements in Microsoft Excel. To confirm these results, the nTA measurements were aggregated into 1 km^2 increments moving out from the carbonate island or atoll. The surface mix layer mean nTA values of each 1 km^2 bin were compared with the open ocean references to determine to what distance the difference extends (Figure 3). A series of pairwise t tests were completed using PC-ORD 6.19 to determine which mean nTA values for each 1 km^2 distance bin were statistically different from either of the open ocean references.

To assess symmetry, the mean nTA for 63 discrete samples collected from the surface mix layer during five southwest (SW) and five northeast (NE) transects were compared for Pearl and Hermes Atoll. A best fit regression (highest R^2) was utilized to determine the distance beyond the 25 m isobath at which the mean nTA values were equivalent to the open ocean reference values. To confirm these results, the data were aggregated into 1 km^2 increments moving out from the 25

m isobath at Pearl and Hermes Atoll to compare the mean values. The surface mix layer mean nTA values of each 1 km^2 bin in the SW and NE directions were compared with distance from the 25 m isobath (Figure 4). A series of pairwise t tests were completed across the distance bins to determine statistical differences between the mean nTA values moving out in the southwest or northeast direction from Pearl and Hermes Atoll.

2.2.e Analysis of Hawaiian Archipelago Gradient

To characterize the gradient along the Main and Northwestern Hawaiian Island archipelago, the surface mix layer nTA measurements collected during the southwest transects within 2.5 km from the 25 m isobath of each carbonate island or atoll were compared using the Lo'ihi Seamount at the southeastern most point of the archipelago as a distance reference. The straight-line distance from Lo'ihi Seamount was calculated for each CTD hydrocast's latitude and longitude (http://www.soest.hawaii.edu/GG/HCV/loihi.html). The measured nTA within 2.5 km of the 25 m isobath were fit with the best (highest R^2) regression to the distance from Lo'ihi Seamount.

To interpret the change in IME along the Hawaiian Archipelaog, a 'biogeophysical factor' was created to interpret the influence of three parameters, mean solar radiation, summertime surface current, and shallow area, on the alkalinity deficit measured at each NWHI (Table 3) (Gove et al. 2016). The three parameters were reduced to fractional values of each parameter's maximum in the NWHI. Then, each NWHI's 'biogeophysical factor' was calculated as the average of these three fractional values. The mean daily solar radiation which linearly decreases (R^2 = 0.0849) moving up the NWHI Archipelago was used to approximate changes in the light enhanced calcification rate (Grigg 1981,1983). The residence time was estimated from the volumetric flow rate and distance traveled through each carbonate island or atoll. The volumetric flow rate was

approximated from the mean daily Hybrid Coordinate Ocean Model (HYCOM) surface current from three to five coordinates surrounding each NWHI on June 15th, July 15th, August 15th, and September 15th of 2012 surrounding each NWHI. The mean summertime residence time varies by NWHI, generally increasing moving up the archipelago with the exception of a slight decrease around Pearl and Hermes Atoll. The shallow area was calculated as the area of the carbonate island or atoll platform less than 30 m deep (Gove et al. 2013). Atolls have the largest area of shallow habitat, which are mid-archipelago in the NWHI (Grigg 1983; Gove et al. 2013).

2.2.f Alkalinity Deficit Calculations at French Frigate Shoals

The alkalinity difference between the nearshore waters of French Frigate Shoals and the open ocean was used along with the volume and seawater density associated with the alkalinity deficit to compute a molar quantity of alkalinity removed.

$$Alkalinity\ Deficit\ (\mu mol) = Avg(nTA_x - nTA_{open\ ocean})(\frac{\mu mol}{kg}) \times V(vol.) \times \rho_{SW}(\frac{mass}{vol.}) \quad (1)$$

To quantify the alkalinity deficit at French Frigate Shoals, normalized alkalinity measured in the nearshore surface waters across all years from the southwest transects was compared to the open ocean references. The FFS reef ecosystem was delineated by the distance limit of the mean nTA deficit which encompassed the region where 123 discrete seawater samples were collected (Figure 5). The FFS seawater volume was divided into mutually exclusive volumes, each with an unique carbonate chemistry concentration. First, the FFS volume was portioned vertically as the surface mixed layer and the subthermocline to 100 dbar depth. Then, the FFS volume was portioned radially at the 25 m isobath and the maximum distance with a mean nTA deficit. At FFS this distance was ~9.6 km beyond the 25 m isobath. The total alkalinity removed from the seawater moving across FFS was estimated as the summation of the mean nTA deficits of all four FFS seawater volumes.

Seawater volume and density were used to convert the nTA deficit concentration into a molar quantity of alkalinity removed from the FFS seawater system. The seawater volume estimate was generated using ArcGIS 10.2.2 Spatial Analyst based on bathymetry maps from the Pacific Islands Benthic Habitat Mapping Center gridded at 5 m for French Frigate Shoals. The seawater density for each volume was estimated as the mean CTD measurement adjusted to remove the impact of salinity on density using the Thermodynamic Equation of State (TEOS) 10 program to avoid accounting for salinity differences more than once in the alkalinity deficit calculation (Pawlowicz 2010; Wright et al. 2011).

2.2.g Net $CaCO_3$ Production at French Frigate Shoals

For each mole of calcium carbonate precipitated the ionic charge or nTA of the seawater decreased by two, therefore one half of the change in nTA was used to calculate the amount of calcium carbonate produced (Zeebe and Wolf-Gladrow 2001; Shamberger et al. 2011; Zeebe and Ridgwell 2011; Lantz et al. 2013). The molecular weight of calcium carbonate, 100.09 g/mol, was used to convert from a molar quantity of alkalinity to mass of $CaCO_3$.

Further quantifying the calcium carbonate precipitation by a residence time and vertical accretion area generates an estimate of the net calcification rate at FFS. The residence time, Δt calculated using equation 2, was estimated as the average seawater transit time the volume of water impacted by the IME around FFS (V) divided by the volumetric surface flow rate (Q).

$$\Delta t\ (yr) = V(km^3) \div Q\left(\frac{km^3}{yr}\right) \quad (2)$$

The volumetric flow rate, Q, was approximated from the mean HYCOM surface current of 12 coordinates northeast of the atoll from June 1st through September 30th, 2012 along with the bathymetry of FFS (Figure 6). The 2012 mean monthly summertime surface current of 15.7 cm/s was used, because HYCOM model data were not available preceding February 2012 for FFS. The

surface current was approximated using the resultant velocity vector of the eastward and northward HYCOM + NCODA 1/12° reanalysis seawater velocity. The daily mean surface current values were tabulated from the HYCOM model surrounding French Frigate Shoals within 23.80 to 24.65°N and 165.65 to 166.10°W from June 1 and September 30, 2012.

The surface area at FFS as a function of depth was computed to approximate the 'island area' subject to vertical accretion (Figure 7). In the Au'au Channel, 50 m depth is expected to be the maximum depth coral reef accretion exceeds erosion (Grigg 2006; Sheppard et al. 2009). The slope of the shelf beyond the 35 m isobath at FFS is extremely steep, therefore increasing the estimate of the island size does not add significant area that would contribute to vertical accretion. An estimate of 184 km^2 inside the 35 m isobaths at FFS was generated using ArcGIS 10.2.2 Spatial Analyst based on bathymetry maps from the Pacific Islands Benthic Habitat Mapping Center gridded at 5 m.

$$Calcification\ Rate\left(\frac{kg}{\frac{m^2}{yr}}\right) = \frac{Alkalinity\ Deficit\ (\mu mol)}{Island\ Area\ (km^2)\ \times\ \Delta t(yr)} \times \frac{1\ carbon\ \left(\frac{\mu mol}{kg}\right)}{2\ alkalinity\ \left(\frac{\mu mol}{kg}\right)} \times MW_{CaCO_3}\left(\frac{kg}{\mu mol}\right) \quad (3)$$

2.2.h Seasonal Difference in Calcification Rate

Peak calcification rates have been reported during the summer months for subtropical reef ecosystems (Table 4) (Bates et al. 2010; Shaw and McNeil 2014; Yeakel et al. 2015). To adjust the summertime net calcification rate to reflect the annual average, the mean NEC and nTA deficit values reported at three subtropical reefs for summertime (June through August) and year-round were compared to determine the ratio of the annual to summertime net $CaCO_3$ production rate.

2.2.i Vertical Atoll Accretion Rate Calculation at French Frigate Shoals

The calcification rate of French Frigate Shoals' nearshore reef ecosystem along with approximations for the 'bulk island density' and carbonate island carbon composition were used

to compute the vertical accretion rate across FFS' island platform.

$$Island\ Accretion\ \left(\frac{mm}{yr}\right) = \frac{Calcification\ Rate\ \left(\frac{\frac{kg}{m^2}}{yr}\right)\ x\ 1000\ (\frac{mm}{m})}{\%\ CaCO_3\ of\ Coral\ Island \times Bulk\ Island\ Density\ (\frac{kg}{m^3})} \quad (4)$$

The 'bulk island density' was estimated as 1.48 mg/mm^3. This value is the mean of the measured coral density at FFS of 1.4 mg/mm^3 and mean bulk coralline algae density in Barbados of 1.56 mg/mm^3 (Stearn et al. 1977; Grigg 1982; Harney and Fletcher III 2003). A conservative estimate of the organic matter and voids of 0.1 wt% was applied to the estimate, which reduced the 'bulk island density' slightly (Ingalls et al. 2003; Watanabe et al. 2003; Muscatine et al. 2004).

2.2.j Propagation of Error of Atoll Accretion Rate

To account for the propagation of error from the estimates used to compute the atoll accretion rate at French Frigate Shoals, the standard deviation of each input was used to calculate the total error associated with the net $CaCO_3$ production rates and the vertical reef accretion rates.

$$Calculation\ of\ Error\ Propagation, st.dev.$$

$$x = \frac{a \cdot b}{c} \longrightarrow \frac{\sigma_x}{x} = \sqrt{[(\frac{\sigma_a}{a})^2 + (\frac{\sigma_b}{b})^2 + (\frac{\sigma_c}{c})^2]} \quad (5)$$

The potential error associated with the accretion rates was calculated using the standard deviation of the input parameters. The standard deviation of the 120 days of daily mean HYCOM surface velocity averaged across 12 coordinates northeast of FFS was used to calculate the standard deviation for the surface current factor. The seawater density standard deviation was estimated using TEOS10 with the precision values for the CTD temperature (+/- 0.001 °C) and salinity (+/- 0.003 PSU) as inputs (Pawlowicz 2010). The 'bulk island density' standard deviation was approximated using the coral core density repeatability measured using scanning densitometer (Lough and Barnes 1997). The standard deviation for the 'island area' was calculated using a 5 m horizontal resolution for the bathymetry maps from the Pacific Islands

Benthic Habitat Mapping Center. Seawater volume standard deviation was calculated using a 5 m horizontal resolution and 0.01 m depth resolution for the bathymetry maps from the Pacific Islands Benthic Habitat Mapping Center.

2.3 Results

2.3.a Northwestern Hawaiian Islands Spatial Analysis

Significantly depleted normalized total alkalinity was observed in the nearshore surface waters of the Northwestern Hawaiian Islands compared to HOT and WOCE (Figure 8). Along the NWHI, several carbonate islands and atolls show a normalized total alkalinity deficit compared to the open ocean surface values stretching out between 7.0 and 23.4 km (Table 5). A clear, persistent alkalinity deficit was observed in the nearshore waters of French Frigate Shoals (FFS) compared to the open ocean surface values to a distance of ~23.4 km from FFS center or 9.6 km from the 25 m isobath (Figure 9). When the data are binned in 1 km^2 intervals at FFS, an alkalinity deficit of ~22 μmol/kg was measured within the 25 m isobath which was nearly significantly different from the open ocean values, $p<0.10$ (Figure 10). The nearshore waters of the NWHI had statistically different normalized total alkalinity compared to the open ocean for sigma theta depth bins less than 24.0 kg/m^3 sigma theta or the upper 100 dbar (Figure 11 & 12).

2.3.b Symmetry at Pearl and Hermes Atoll

Mean nTA did not show a strong statistically significant relationship with distance from the center of Pearl and Hermes in the northeast (NE) or southwest (SW) transects. In addition, the mean values in the NE and SW direction were not statistically different (Figure 13).

2.3.c Hawaiian Archipelago Gradient

Along the Hawaiian Archipelago a parabolic like trend of mean nTA within 2.5 km of the 25 m isobaths was observed of a maximum mean nTA at the island of Hawaii, a minimum at Maro

Reef, and a maximum was northward at Kure and Midway Atolls (Figure 14). A comparison of mean nTA and total variance of the surface mixed layer within 2.5 km of the 25 m isobath southwest of the Hawaiian Islands indicates no one Main or Northwestern Hawaiian Island was statistically different in nTA from the rest ($p = 0.50$) (Figure 15).

2.3.d Net $CaCO_3$ Production and Vertical Atoll Accretion at French Frigate Shoals

An instantaneous net alkalinity deficit of 8.9×10^{14} μmoles was observed at FFS compared to the surface waters of HOT station ALOHA (Table 6). Applying the snapshot deficit over the residence time of seawater moving across the FFS platform a net $CaCO_3$ production rate of 9.6 +/- 2.8 kg/m^2/yr (96,176,040 +/- 28,051,345 μmol/m^2/yr) was computed using equation (3). Using equation (4), the average vertical accretion rate calculated for the French Frigate Shoals (FFS) atoll platform was 10.0 +/- 2.9 mm/yr (Table 6).

Two variables were examined to assess their impact on the final reef accretion rate estimation (Table 7). To evaluate the impact of monthly and interannual variability on the reef accretion rate, the monthly mean HYCOM surface currents of each summertime month from June through September 2012 were compared. The mean monthly surface current ranged from a minimum of 11.2 cm/s in July 2012 to a maximum of 21.3 cm/s in August, which resulted in reef accretion rates of -29% and +36% of the mean, respectively.

The ‘bulk island density’ value used has a large impact on the estimated vertical reef accretion at French Frigate Shoals. If the *Porites lobata* coral core density has been measured at French Frigate Shoals at 1.2 mg/mm^3 (Grigg 1981) and the maximum possible ‘bulk island density’ equivalent to packed Oahu beach sand of 1.71 mg/mm^3 (Hardisty 1990; Smith and Cheung 2002) the use of these values resulted in a FFS atoll accretion rate +17% or -18% of the mean, respectively. When the ‘island area’ at French Frigate Shoals was modified to include the

shelf to a depth of 100 m, FFS atoll accretion rate declined by ~22%. The vertical reef accretion rate estimate varied less than 0.015% when different seawater density values were used (average CTD, average of upper 10 m at HOT station ALOHA from 2009 to 2012 between June and September, versus average TEOS10 standardized seawater density).

2.3.e Quality Assessment

Replicate measurement of nTA indicated the average difference amongst duplicate alkalinity measurements was 4.02 μmol/kg with a standard deviation of 4.06 μmol/kg computed in accordance with the DOE manual (Dickson et al. 2007) (Table 2). The average mean difference of the Certified Reference Materials (CRMs) provided by Scripps Institution of Oceanography and Pacific Marine Environmental Laboratory (PMEL) measured from the reported alkalinity value was 3.97 μmol/kg with a standard deviation of 4.87 μmol/kg.

2.4 Discussion

2.4.a Archipelago Wide Alkalinity Deficit Halo

The archipelago wide alkalinity deficit halo observed in the nearshore surface seawater surrounding the NWHI indicates the reef ecosystem is net calcifying (Smith and Kinsey 1978; Smith et al. 1978; Chisholm and Gattuso 1991; Shamberger et al. 2011; Venti et al. 2012). Vertical limestone accretion has offset the ~120 m rise in sea level in the past 19,000 years maintaining the NWHI as subaerial edifices (Gross et al. 1969; Ladd et al. 1970; Grigg 1982; Grigg and Epp 1989; Rooney et al. 2008). [SK5]

While moving northward along the NWHI Archipelago, light enhanced calcification rate decreases while shallow reef habitat and residence time increases thereby cumulating mid-archipelago between French Frigate Shoals and Maro Reef in a maximum alkalinity deficit (Table 8). [SK6]The calculated ‘biogeophysical factor’ accounted for ~75% of the variance in the magnitude

of the mean nTA measured at each NWHI (Figure 16). Underway pH and pCO_2 data collected in the NWHI in 2010 and 2011 showed consistent results indicating the strongest calcification signal in the nearshore waters of French Frigate Shoals, Gardner Pinnacles, Maro Reef, and Pearl and Hermes Atoll (Kealoha et al. 2015). The spatial extent of the alkalinity deficit was consistent with elevated pCO_2 surrounding the NWHI which ranged between 10 to 20 km away from the atoll (Kealoha et al. 2015). In addition, the alkalinity deficit was also consistent with elevated phytoplankton concentration within 30 km of the shoreline (Gove et al. 2016). The same drivers promoting high nearshore phytoplankton biomass also drive greater abundance of reef-building marine calcifiers (Williams et al. 2015; Gove et al. 2016). Calcification is strongest near the surface and attenuates rapidly with increasing depth as the increasing seawater volume dilutes the metabolic signal. The alkalinity deficit halo extends from the surface to the depth [SK7]of vertical mixing, typically about 100 m (Baker and Weber 1975; Highsmith 1979; Huston 1985; Grigg and Epp 1989; Brainerd and Gregg 1995; Karl 1999; Sheppard et al. 2009; Sorek and Levy 2012; Smith and Mackenzie 2015).

Whereas earlier studies appear to be contrary to net calcification around the NWHI, there are potential explanations consistent with our conclusions. [SK8]Sabine and Mackenzie (1995) detected an alkalinity surplus or 'halo' that was strongest in deep water and weakened in the surface waters. The results were consistent with our data but with an offset likely because they did not have a certified reference material (Thompson et al. 2014). Thompson et al. (2014) revisited the alkalinity 'halo' theory using the 2009 data set of this analysis but did not detect an alkalinity deficit. However, the data set did not include sufficient shallow water samples, where the signal is strongest, to draw a robust conclusion.

2.4.b Net $CaCO_3$ Production and Vertical Atoll Accretion at French Frigate Shoals

Our observations suggest a net $CaCO_3$ production rate of about 9.6 kg/m^2/yr at French Frigate Shoals. This estimate is a summertime value and may not reflect the year-round average. On a Bermuda reef flat at ~32°N, net ecosystem calcification (NEC) and the nTA deficit was roughly twice as great in the summer as the rest of the year (Bates et al. 2010; Yeakel et al. 2015). Similarly, results from the southern Great Barrier Reef at ~24°S showed the summer season nTA deficit was roughly twice as great as the other seasons (Shaw and McNeil 2014). However, it is important to note that residence time may additionally impact NEC seasonally. Adjusting the estimation of the FFS summertime net $CaCO_3$ production rate to account for seasonal variability reduces the rate by a factor of 0.69 to produce an annualized net $CaCO_3$ rate of 6.6 kg/m^2/yr.

Two fundamental assumptions are critical to our estimate of net calcification. First, our analysis assumes that the coastal ocean exhibits no diel pattern in alkalinity deficit due to horizontal mixing and second, our analysis assumes that nTA displays radial symmetry about the atoll. There was no evidence of a diel cycle in the CO_2-carbonic-acid system at FFS as distance from the shallow reef appeared to have the greatest impact on the carbon chemistry. Taking into account mean monthly summertime HYCOM surface current estimations and the distance covered at FFS, the equivalent temporal sampling coverage encompassed the full diel cycle. The off-reef nTA measurement represented a well mixed atoll platform signal not the diel oscillations observed on reef (Venti et al. 2012; Lantz et al. 2013; Kealoha et al. 2015). An equivalent magnitude of the alkalinity deficit halo was observed up current and down current of Pearl and Hermes. Instantaneous eddy fields can be greater than average eddy fields causing dissipation in directions other than the predominant surface current despite unidirectional advection through a system (Imberger et al. 1983; Hatcher et al. 1987). Symmetry in the carbonate parameters was consistent

with radially symmetrical Chlorophyll concentration measurements previously reported at the atoll to a distance of 16 km in all directions (Gove et al. 2013).

Globally census-based studies typically report net $CaCO_3$ production rates for individual reef or island wide surveys that are slightly lower than our estimation for FFS but within the same order of magnitude (Table 9) (Harney and Fletcher III 2003; Silverman et al. 2012; Perry et al. 2013). The census-based approach may not capture all benthic contributors or characterize the level of rugosity or surface relief of all species and benthic cover which impact the calcification rate with visual assessment especially species like foraminifera, *Halimeda*, or molluscs (Yamano et al. 2005; Perry et al. 2013). Benthic foraminifera can be the major contributor to $CaCO_3$ production for an ecosystem as observed in the nearshore reef ecosystem of Majuro Atoll in the Marshall Islands (Emery 1956; Yamano et al. 2005). Globally hydrochemical studies of individual reefs are consistent with our atoll scale approximation (Table 9) (Suzuki et al. 1995; Gattuso et al. 1996; Shamberger et al. 2011; Venti et al. 2012; Albright et al. 2013; Lantz et al. 2013).

There are several explanations for the high calcification rate measured at French Frigate Shoals. French Frigate Shoals had the highest percent coral cover reported in the Hawaiian Archipelago (Grigg 1981). Coral reef and crustose coralline algae have the two highest calcification rates of species studied on Hawaiian reefs (Chave et al. 1972; Agegian 1985; Grossman 2001; Harney and Fletcher III 2003). The majority of census-based and hydrochemical reef assessments occur above shallow coral reef flats but may overlook areas with the highest calcification such as the reef crest or depths around 10 m (Grigg and Epp 1989; Falter et al. 2005; Perry et al. 2013).

The vertical atoll accretion rate for French Frigate Shoals of 10.0 mm/yr is an estimation of the summertime average. Annualizing the summertime vertical atoll accretion rate at French

Frigate Shoals reduces the rate by a factor of 0.69 to 6.9 mm/yr. Adjusting for carbon export from the platform shelf by major storms further reduces the platform accretion rate by roughly 25% to 5.2 mm/yr (Land 1979; Hine et al. 1981; Sadd 1984; Hubbard et al. 1990; Hubbard 1992; Harney and Fletcher III 2003). Studies of individual reef accretion rates in the North Pacific subtropics using the hydrochemical approach have values close to our approximation but are generally slightly lower (Table 9) (Ohde and van Woesik 1999; Shamberger et al. 2011; Lantz et al. 2013).

Historically, net $CaCO_3$ production has exceeded sea level rise, carbon export off the platform shelf, and plate subsidence, which enables the maintenance of subaerial habitat in the NWHI. Sea level rise in the North Pacific basin is projected to increase by ~6 mm/yr through the remainder of the 21st century (Church et al. 2013; Edenhofer et al. 2014; Field and Van Aalst 2014; Kench et al. 2015). Our calculation is consistent with other studies that concluded French Frigate Shoals calcium carbonate vertical deposition has historically kept pace with sea level rise but may not in the future. Accelerated sea level rise may cause measurable change in the reef habitat at FFS over the next couple hundred years as increasing surface seawater warming and ocean acidification intensify stress on marine calcifiers which may decrease calcification and increase dissolution (Andersson et al. 2003; Andersson et al. 2005; Siciliano 2005; Morse et al. 2006; Andersson et al. 2007; Baker et al. 2007; Kuffner et al. 2007; Grigg et al. 2008a; Rooney et al. 2008; Perry et al. 2012).

Our approach is novel using hydrochemical analysis on a carbonate island or atoll scale to address habitat viability in the face of accelerated sea level rise. There are opportunities to improve the utility of this approach with improved oceanographic measurements during sample collection to eliminate the need to infer surface current and residence time from independent data collection or modeling (Venti et al. 2012). As well as more sampling both up and down current of the

predominant current to have greater confidence that the carbonate parameters demonstrate symmetry about the carbonate island or atoll. The vertical carbonate island or atoll accretion rate hinges on an approximation of island density from coral and coralline algae cores and would improve with direct measurement of these parameters. Additionally, diel sampling throughout the year as well as sediment trap deployments would eliminate the need for the many caveats described in this paper. These results can provide vital insight into whether the NWHI will remain viable nesting and rearing habitat for endangered and threatened species like the Hawaiian monk seal, green sea turtle, and several seabirds (Andréfouët and Payri 2001; Baker et al. 2007). This approach can be used before and after changes in community composition to evaluate the effect of the observed changes on community metabolic rates and easily adapted to other carbonate islands and atolls to estimate long term viability of habitat for protected species and human populations which rely on the reef for survival (Kayanne et al. 2005; Shaw et al. 2016).

Works Cited

(PSMSL) PSFMSL (2016) Tide Gauge Data, http://www.psmsl.org/data/obtaining/.

Agegian CR (1985) The biogeochemical ecology of Porolithon gardineri Unpublished PhD thesis, Department of Oceanography, University of Hawaii, Honolulu, 178 p

Albright R, Langdon C, Anthony KRN (2013) Dynamics of seawater carbonate chemistry, production, and calcification of a coral reef flat, central Great Barrier Reef. Biogeosciences 10:6747-6758

Albright R, Mason B, Miller M, Langdon C (2010) Ocean acidification compromises recruitment success of the threatened Caribbean coral Acropora palmata. Proceedings of the National Academy of Sciences 107:20400-20404

Andersson AJ, Mackenzie FT (2004) Shallow-water oceans: a source or sink of atmospheric CO2? Frontiers in Ecology and the Environment 2:348-353

Andersson AJ, Gledhill D (2012) Ocean Acidification and Coral Reefs: Effects on Breakdown, Dissolution, and Net Ecosystem Calcification. Annual Review of Marine Science

Andersson AJ, Mackenzie FT, Ver LM (2003) Solution of shallow-water carbonates: An insignificant buffer against rising atmospheric CO2. Geology 31:513-516

Andersson AJ, Mackenzie FT, Lerman A (2005) Coastal ocean and carbonate systems in the high CO2 world of the Anthropocene. American Journal of Science 305:875-918

Andersson AJ, Bates NR, Mackenzie FT (2007) Dissolution of carbonate sediments under rising pCO2 and ocean acidification: observations from Devil's Hole, Bermuda. Aquatic Geochemistry 13:237-264

Andersson AJ, Kline DI, Edmunds PJ, Archer SD, Bednaršek N, Carpenter RC, Chadsey M, Goldstein P, Grottoli AG, Hurst TP (2015) Understanding ocean acidification impacts on organismal to ecological scales. Oceanography 28

Andréfouët S, Payri C (2001) Scaling-up carbon and carbonate metabolism of coral reefs using in-situ data and remote sensing. Coral Reefs 19:259-269

Baker JD, Littnan CL, Johnston DW (2007) Potential effects of sea level rise on the terrestrial habitats of endangered and endemic megafauna in the Northwestern Hawaiian Islands. Endangered Species Research 3:21-30

Baker PA, Weber JN (1975) Coral growth rate: variation with depth. Physics of the Earth and Planetary Interiors 10:135-139

Bates N, Astor Y, Church M, Currie K, Dore J, Gonaález-Dávila M, Lorenzoni L, Muller-Karger F, Olafsson J, Santa-Casiano M (2014) A time-series view of changing ocean chemistry due to ocean uptake of anthropogenic CO2 and ocean acidification. Oceanography 27:126-141

Bates NR, Michaels AF, Knap AH (1996) Seasonal and interannual variability of oceanic carbon dioxide species at the US JGOFS Bermuda Atlantic Time-series Study (BATS) site. Deep Sea Research Part II: Topical Studies in Oceanography 43:347-383

Bates NR, Amat A, Andersson AJ (2010) Feedbacks and Responses of coral calcification on the Bermuda Reef system to seasonal changes in biological processes and ocean acidification. Biogenesis 7:2509-2530

Boland RC, Donohue MJ (2003) Marine debris accumulation in the nearshore marine habitat of the endangered Hawaiian monk seal, Monachus schauinslandi 1999–2001. Marine Pollution Bulletin 46:1385-1394

Brainerd KE, Gregg MC (1995) Surface mixed and mixing layer depths. Deep Sea Research Part I: Oceanographic Research Papers 42:1521-1543

Brix H, Gruber N, Keeling CD (2004) Interannual variability of the upper ocean carbon cycle at station ALOHA near Hawaii. Global Biogeochemical Cycles 18:GB4019

C. L. Sabine FTM (1995) Bank-derived carbonate sediment transport and dissolution in the Hawaiian Archipelago. Aquatic Geochemistry 1:189-230

Caldeira K, Wickett ME (2003) Oceanography: anthropogenic carbon and ocean pH. Nature 425:365-365

Chave KE, Smith SV, Roy KJ (1972) Carbonate production by coral reefs. Marine Geology 12:123-140

Chisholm JRM, Gattuso JP (1991) Validation of the alkalinity anomaly technique for investigating calcification of photosynthesis in coral reef communities. Limnology and Oceanography 36:1232-1239

Church JA, White NJ, Hunter JR (2006) Sea-level rise at tropical Pacific and Indian Ocean islands. Global and Planetary Change 53:155-168

Church JA, White NJ, Coleman R, Lambeck K, Mitrovica JX (2004) Estimates of the regional distribution of sea level rise over the 1950-2000 period. Journal of Climate 17:2609-2625

Church JA, Clark PU, Cazenave A, Gregory JM, Jevrejeva S, Levermann A, Merrifield M, Milne G, Nerem R, Nunn P (2013) Sea level change. Climate change:1137-1216

Clayton TD, Byrne RH (1993) Spectrophotometric seawater pH measurements: total hydrogen ion concentration scale calibration of m-cresol purple and at-sea results. Deep Sea Research Part I: Oceanographic Research Papers 40:2115-2129

Cyronak T, Santos IR, McMahon A, Eyre BD (2013) Carbon cycling hysteresis in permeable carbonate sands over a diel cycle: Implications for ocean acidification. Limnol Oceanogr 58:131-143

Desch A, Wynne T, Brainard R, Friedlander A, Christensen J (2009) Oceanographic and Physical Setting. A Marine Biogeographic Assessment of the Northwestern Hawaiian Islands:17

Dickson AG, Goyet C (2005) Handbook of methods for the analysis of the various parameters of the carbon dioxide system in sea water. publisher not identified

Dickson AG, Sabine CL, Christian JR (2007) Guide to best practices for ocean CO2 measurements

Dore JE, Lukas R, Sadler DW, Karl DM (2003) Climate-driven changes to the atmospheric CO2 sink in the subtropical North Pacific Ocean. Nature 424:754-757

Dore JE, Lukas R, Sadler DW, Church MJ, Karl DM (2009) Physical and biogeochemical modulation of ocean acidification in the central North Pacific. Proceedings of the National Academy of Sciences 106:12235-12240

Doty MS, Oguri M (1956) The island mass effect. Journal du Conseil 22:33-37

Drupp PS, De Carlo EH, Mackenzie FT, Sabine CL, Feely RA, Shamberger KE (2013) Comparison of CO2 Dynamics and Air–Sea Gas Exchange in Differing Tropical Reef Environments. Aquatic Geochemistry 19:371-397

Dubinsky Z, Falkowski P (2011) Light as a source of information and energy in zooxanthellate corals Coral Reefs: An Ecosystem in Transition. Springer, pp107-118

Edenhofer O, Pichs-Madrug R, Sokona Y (2014) IPCC 2014: Summary for Policymakers. clim chang:1-32

Emerson S, Hedges J (2008) Chemical oceanography and the marine carbon cycle. Cambridge University Press

Emery K (1956) Marine geology of Johnston Island and its surrounding shallows, central Pacific Ocean. Geological Society of America Bulletin 67:1505-1520

Erez J, Reynaud S, Silverman J, Schneider K, Allemand D (2011) Coral calcification under ocean acidification and global change Coral reefs: an ecosystem in transition. Springer, pp151-176

Eyre BD, Andersson AJ, Cyronak T (2014) Benthic coral reef calcium carbonate dissolution in an acidifying ocean. Nature Climate Change 4:969-976

Fagan KE, Mackenzie FT (2007) Air–sea CO< sub> 2</sub> exchange in a subtropical estuarine-coral reef system, Kaneohe Bay, Oahu, Hawaii. Marine Chemistry 106:174-191

Falter JL, Atkinson MJ, Coimbra CF (2005) Effects of surface roughness and oscillatory flow on the dissolution of plaster forms: Evidence for nutrient mass transfer to coral reef communities. Limnology and oceanography 50:246-254

Falter JL, Lowe RJ, Zhang Z, McCulloch M (2013) Physical and biological controls on the carbonate chemistry of coral reef waters: effects of metabolism, wave forcing, sea level, and geomorphology. PloS one 8:e53303

Feely RA, Allison LJ, Griffith DC (1999) Comparison of the carbon system parameters at the global CO2 survey crossover locations in the North and South Pacific Ocean, 1990-1996. Carbon Dioxide Information Analysis Center

Feely RA, Doney SC, Cooley SR (2009) Ocean Acidification: Present Conditions and Future Changes in a High-CO2 World. Oceanography 22:36-47

Feely RA, Sabine CL, Lee K, Berelson W, Kleypas JA, Fabry VJ, Millero FJ (2004) Impact of anthropogenic CO2 on the CaCO3 system in the oceans. Science 305:362-366

Field CB, Van Aalst M (2014) Climate change 2014: impacts, adaptation, and vulnerability. IPCC

Firing J, Brainard RE (2006) Ten years of shipboard ADCP measurements along the Northwestern Hawaiian Islands. Atoll research bulletin 543:347-364

Fletcher CH, Bochicchio C, Conger CL, Engels MS, Feirstein EJ, Frazer N, Glenn CR, Grigg RW, Grossman EE, Harney JN (2008) Geology of Hawaii reefs Coral Reefs of the USA. Springer, pp435-487

Ford MR, Kench PS (2015) Multi-decadal shoreline changes in response to sea level rise in the Marshall Islands. Anthropocene

Ford MR, Kench PS (2016) Spatiotemporal variability of typhoon impacts and relaxation intervals on Jaluit Atoll, Marshall Islands. Geology 44:159-162

Friedlander AM, DeMartini EE (2002) Contrasts in density, size, and biomass of reef fishes between the northwestern and the main Hawaiian islands: the effects of fishing down apex predators. Marine Ecology Progress Series 230:253-264

Friedlander AM, Keller K, Wedding L, Clarke A, Monaco M (2009) A marine biogeographic assessment of the Northwestern Hawaiian Islands. Citeseer

Friedlander AM, Maragos J, Brainard R, Clark A, Aeby G, Bowen B, Brown E, Chaston K, Kenyon J, Meyer C, McGowen P, Miller J, Montgomery T, Schroeder R, Smith C, Vroom P, Walsh W, Williams I, Wiltse W, Zamzow J (2008) Status of Coral Reefs in Hawaii and United States Pacific Remote Island Areas (Baker, Howland, Palmyra, Kingman, Jarvis, Johnston, Wake) in 2008. Status of Coral Reefs of the World: 2008

Garbe CS, Rutgersson A, Boutin J, de Leeuw G, Delille B, Fairall CW, Gruber N, Hare J, Ho DT, Johnson MT (2014) Transfer Across the Air-Sea Interface Ocean-Atmosphere Interactions of Gases and Particles. Springer, pp55-112

Gattuso JP, Hansson L (2011) Ocean acidification: background and history. Ocean acidification:1-20

Gattuso JP, Pichon M, Delesalle B, Canon C, Frankignoulle M (1996) Carbon fluxes in coral reefs. I. Lagrangian measurement of community metabolism and resulting air-sea CO~ 2 disequilibrium. MARINE ECOLOGY-PROGRESS SERIES 145:109-121

Gattuso JP, Bijma J, Gehlen M, Riebesell U, Turley C (2011) Ocean acidification: knowns, unknowns, and perspectives. Ocean acidification 2:291

Gehlen M, Gruber N, Gangsto R, Bopp L, Oschlies A (2011) Biogeochemical consequences of ocean acidification and feedbacks to the earth system. Ocean acidification:230-248

Gove JM, Williams GJ, McManus MA, Heron SF, Sandin SA, Vetter OJ, Foley DG (2013) Quantifying Climatological Ranges and Anomalies for Pacific Coral Reef Ecosystems. PLoS ONE 8:1-14

Gove JM, McManus MA, Neuheimer AB, Polovina JJ, Drazen JC, Smith CR, Merrifield MA, Friedlander AM, Ehses JS, Young CW (2016) Near-island biological hotspots in barren ocean basins. Nature communications 7

Gran G (1952) Determination of the equivalence point in potentiometric titrations of seawater with hydrochloric acid. Oceanol Acta 5:209-218

Grigg RW (1981) Coral reef development at high latitudes in Hawaii. Proc 4th Int Coral Reef Symp 1:687-693

Grigg RW (1982) Darwin Point: a threshold for atoll formation. Coral reefs 1:29-34

Grigg RW (1983) Community structure, succession and development of coral reefs in Hawaii. A Natural History of the Hawaiian Islands: Selected Readings II:196

Grigg RW (2006) Depth limit for reef building corals in the Au'au Channel, SE Hawaii. Coral Reefs 25:77-84

Grigg RW, Epp D (1989) Critical depth for the survival of coral islands: effects on the Hawaiian Archipelago. Science 243:638-641

Grigg RW, Wells JW, Wallace C (1981) Acropora in Hawaii. Part 1. History of the Scientific Record, Systematics, and Ecology. Pacific Science 35

Grigg RW, Polovina J, Friedlander AM, Rohmann SO (2008a) Biology of coral reefs in the Northwestern Hawaiian Islands Coral reefs of the USA. Springer, pp573-594

Grigg RW, Polovina J, Friedlander J, Alan M, Rohmann SO (2008b) Biology of coral reefs in the Northwestern Hawaiian Islands Coral reefs of the USA. Springer, pp573-594

Gross MG, Milliman JD, Tracey Jr JI, Ladd HS (1969) Marine geology of Kure and Midway Atolls, Hawaii: a preliminary report

Grossman EE (2001) Holocene sea level history and reef development in Hawaii and the central Pacific Ocean PhD Dissertation: Department of Geology and Geophysics, Univeristy of Hawaii, 257 p

Guinotte JM, Fabry VJ (2008) Ocean acidification and its potential effects on marine ecosystems. Annals of the New York Academy of Sciences 1134:320-342

Hallock P (1981) Production of carbonate sediments by selected large benthic foraminifera on two Pacific coral reefs. Journal of Sedimentary Research 51

Hardisty J (1990) Beaches: form and process. Springer Science & Business Media

Harney J, Fletcher III C (2003) A budget of carbonate framework and sediment production, Kailua Bay, Oahu, Hawaii. Journal of Sedimentary Research 73:856-868
Hart DE, Kench PS (2007) Carbonate production of an emergent reef platform, Warraber Island, Torres Strait, Australia. Coral Reefs 26:53-68
Hatcher BG, Imberger J, Smith SV (1987) Scaling analysis of coral reef systems: an approach to problems of scale. Coral Reefs 5:171-181
Heywood KJ, Barton ED, Simpson JH (1990) The effects of flow disturbance by an oceanic island. Journal of Marine Research 48:55-73
Highsmith RC (1979) Coral growth rates and environmental control of density banding. Journal of Experimental Marine Biology and Ecology 37:105-125
Hine AC, Wilber RJ, Bane JM, Neumann AC, Lorenson KR (1981) Offbank transport of carbonate sands along open, leeward bank margins: northern Bahamas. Marine Geology 42:327-348
Hubbard DK (1992) Hurricane-induced sediment transport in open-shelf tropical systems--an example from St. Croix, US Virgin Islands. Journal of Sedimentary Research 62
Hubbard DK (1997) Reefs as dynamic systems. Life and death of coral reefs:43-67
Hubbard DK, Miller AI, Scaturo D (1990) Production and cycling of calcium carbonate in a shelf-edge reef system (St. Croix, US Virgin Islands): applications to the nature of reef systems in the fossil record. Journal of Sedimentary Research 60
Hughes TP, Baird AH, Bellwood DR, Card M, Connolly SR, Folke C, Grosberg R, Hoegh-Guldberg O, Jackson JBC, Kleypas JA (2003) Climate change, human impacts, and the resilience of coral reefs. science 301:929-933
Huston M (1985) Variation in coral growth rates with depth at Discovery Bay, Jamaica. Coral Reefs 4:19-25
Imberger J, Berman T, Christian R, Sherr E, Whitney D, Pomeroy L, Wiegert R, Wiebe W (1983) The influence of water motion on the distribution and transport of materials in a salt marsh estuary1. Limnology and Oceanography 28:201-214
Ingalls AE, Lee C, Druffel ER (2003) Preservation of organic matter in mound-forming coral skeletons. Geochimica et Cosmochimica Acta 67:2827-2841
Jokiel PL, Jury CP, Ku'ulei SR (2014) Coral-algae metabolism and diurnal changes in the CO2-carbonate system of bulk sea water. PeerJ 2:e378
Jones NS, Ridgwell A, Hendy EJ (2015) Evaluation of coral reef carbonate production models at a global scale. Biogeosciences 12:1339-1356
Juvik SP, Juvik JO, Paradise TR (1998) Atlas of Hawai'i. University of Hawaii Press
Karl DM (1999) A sea of change: Biogeochemical variability in the North Pacific subtropical gyre. Ecosystems 2:181-214
Karl DM, Lukas R (1996) The Hawaii Ocean Time-series (HOT) program: Background, rationale and field implementation. Deep Sea Research Part II: Topical Studies in Oceanography 43:129-156
Kayanne H, Hata H, Kudo S, Yamano H, Watanabe A, Ikeda Y, Nozaki K, Kato K, Negishi A, Saito H (2005) Seasonal and bleaching-induced changes in coral reef metabolism and CO2 flux. Global biogeochemical cycles 19
Kealoha A, Kahng SE, Mackenzie FT, Alin SR, Kosaki RK, Brainard RE, Winn CD (2015) Latitudinal Trends and Drivers in CO2-Carbonic Acid System of Papahānaumokuākea Marine National Monument

Kench P, Thompson D, Ford M, Ogawa H, McLean R (2015) Coral islands defy sea-level rise over the past century: Records from a central Pacific atoll. Geology 43:515-518
Kench PS, Owen SD, Ford MR (2014) Evidence for coral island formation during rising sea level in the central Pacific Ocean. Geophysical Research Letters 41:820-827
Kennedy EV, Perry CT, Halloran PR, Iglesias-Prieto R, Schönberg CH, Wisshak M, Form AU, Carricart-Ganivet JP, Fine M, Eakin CM (2013) Avoiding coral reef functional collapse requires local and global action. Current Biology 23:912-918
Kleypas JA, Langdon C (2006) Coral reefs and changing seawater carbonate chemistry. Coastal and estuarine studies 61:73-110
Kleypas JA, Anthony K, Gattuso JP (2011) Coral reefs modify their seawater carbon chemistry–case study from a barrier reef (Moorea, French Polynesia). Global Change Biology 17:3667-3678
Kleypas JA, Feely RA, Fabry VJ, Langdon C, Sabine CL, Robbins LL (2006) Impacts of Ocean Acidification on Coral Reefs and Other Marine Calcifiers. A Guide for Future Research. Report of a workshop sponsored by NSF, NOAA & USGS
Kuffner IB, Andersson AJ, Jokiel PL, Rodgers KS, Mackenzie FT (2007) Decreased abundance of crustose coralline algae due to ocean acidification. Nature Geoscience 1:114-117
Ladd HS, Tracey JI, Gross MG (1970) Deep drilling on Midway atoll. US Government Printing Office Washington DC
Land LS (1979) The fate of reef-derived sediment on the north Jamaican island slope. Marine Geology 29:55-71
Lantz CA, Atkinson MJ, Winn CD, Kahng SE (2013) Dissolved inorganic carbon and total alkalinity of a Hawaiian fringing reef: chemical techniques for monitoring the effects of ocean acidification on coral reefs. Coral Reefs 10:1-11
Letelier RM, Karl DM, Abbott MR, Bidigare RR (2004) Light driven seasonal patterns of chlorophyll and nitrate in the lower euphotic zone of the North Pacific Subtropical Gyre. Limnology and Oceanography 49:508-519
Lough J, Barnes D (1997) Several centuries of variation in skeletal extension, density and calcification in massive Porites colonies from the Great Barrier Reef: A proxy for seawater temperature and a background of variability against which to identify unnatural change. Journal of Experimental Marine Biology and Ecology 211:29-67
McElligott S, Byrne R, Lee K, Wanninkhof R, Millero F, Feely R (1998) Discrete water column measurements of CO 2 fugacity and pH T in seawater: A comparison of direct measurements and thermodynamic calculations. Marine Chemistry 60:63-73
McMahon A, Santos IR, Cyronak T, Eyre BD (2013) Hysteresis between coral reef calcification and the seawater aragonite saturation state. Geophysical Research Letters 40:4675-4679
Miller CB, Wheeler PA (2012) Biological oceanography. John Wiley & Sons
Millero FJ (2007) The marine inorganic carbon cycle. Chemical reviews 107:308-341
Millero FJ, Lee K, Roche M (1998) Distribution of alkalinity in the surface waters of the major oceans. Marine Chemistry 60:111-130
Milliman J, Müller G, Förstner F (2012) Recent Sedimentary Carbonates: Part 1 Marine Carbonates. Springer Science & Business Media
Morse JW, Arvidson RS (2002) The dissolution kinetics of major sedimentary carbonate minerals. Earth-Science Reviews 58:51-84

Morse JW, Andersson AJ, Mackenzie FT (2006) Initial responses of carbonate-rich shelf sediments to rising atmospheric pCO 2 and “ocean acidification”: role of high Mg-calcites. Geochimica et Cosmochimica Acta 70:5814-5830

Murillo LJA, Jokiel PL, Atkinson MJ (2014) Alkalinity to calcium flux ratios for corals and coral reef communities: variances between isolated and community conditions. PeerJ 2:e249

Muscatine L, Goiran C, Land L, Jaubert J, Guif J-P, Allemand D (2004) Stable isotopes (δ13C and δ15N) of organic matrix from coral skeleton. PNAS 102:1525-1530

Nicholls RJ, Wong PP, Burkett V, Codignotto J, Hay J, McLean R, Ragoonaden S, Woodroffe CD, Abuodha P, Arblaster J (2007) Coastal systems and low-lying areas

NOAA (2015) Ocean Surface Current Analysis - Real Time, www.oscar.noaa.gov

Ohde S, van Woesik R (1999) Carbon dioxide flux and metabolic processes of a coral reef, Okinawa. Bulletin of Marine Science 65:559-576

Pawlowicz R (2010) What every oceanographer needs to know about TEOS-10 (The TEOS-10 Primer). unpublished manuscript, available from www. TEOS-10. org

Perry C, Edinger E, Kench P, Murphy G, Smithers S, Steneck R, Mumby P (2012) Estimating rates of biologically driven coral reef framework production and erosion: a new census-based carbonate budget methodology and applications to the reefs of Bonaire. Coral Reefs 31:853-868

Perry CT (2010) Carbonate Budgets and Reef Framework Accumulation Encyclopedia of Modern Coral Reefs. Springer, pp185-190

Perry CT, Murphy GN, Kench PS, Smithers SG, Edinger EN, Steneck RS, Mumby PJ (2013) Caribbean-wide decline in carbonate production threatens coral reef growth. Nature communications 4:1402

Petit JR, Jouzel J, Raynaud D, Barkov NI, Barnola JM, Basile I, Bender M, Chappellaz J, Davisk M, Delaygue G, Delmotte M, Kotlyakov VM, Legrand M, Lipenkov VY, Lorius C, Pe´ pin L, Ritz C, Saltzmank E, Stievenard M (1999) Climate and atmospheric history of the past 420,000 years from the Vostok ice core, Antarctica. Nature 399:429-436

Polovina JJ, Howell E, Kobayashi DR, Seki MP (2001) The transition zone chlorophyll front, a dynamic global feature defining migration and forage habitat for marine resources. Progress in Oceanography 49:469-483

Rees S, Opdyke B, Wilson P, Henstock T (2007) Significance of Halimeda bioherms to the global carbonate budget based on a geological sediment budget for the Northern Great Barrier Reef, Australia. Coral Reefs 26:177-188

Rooney JJ, Wessel P, Hoeke R, Weiss J, Baker J, Parrish F, Fletcher CH, Chojnacki J, Garcia M, Brainard R (2008) Geology and geomorphology of coral reefs in the Northwestern Hawaiian Islands Coral Reefs of the USA. Springer, pp519-571

Rudnick DL, Boyd TJ, Brainard RE, Carter GS, Egbert GD, Gregg MC, Holloway PE, Klymak JM, Kunze E, Lee CM (2003) From tides to mixing along the Hawaiian Ridge. science 301:355-357

Sabine CL, Mackenzie FT (1995) Bank-Derived Carbonate Sediment Transport and Dissolution in the Hawaiian Archipelago. Aquatic Geochemistry 1:189-230

Sabine CL, Feely RA, Gruber N, Key RM, Lee K, Bullister JL, Wanninkhof R, Wong CSI, Wallace DWR, Tilbrook B (2004) The oceanic sink for anthropogenic CO2. science 305:367-371

Sadd JL (1984) Sediment transport and CaCO3 budget on a fringing reef, Cane Bay, St. Croix, US Virgin Islands. Bulletin of marine science 35:221-238
Sarmiento JL, Gruber N (2006) Ocean Biogeochemical Dynamics. Princeton University Press
Schlanger SO, Konishi K (1975) The geographic boundary between the coral-algal and the bryozoan-algal limestone facies: a paleolatitude indicator. 9th Int Congr Sedimentol, Nice:187-190
Shamberger KEF, Cohen AL, Golbuu Y, McCorkle DC, Lentz SJ, Barkley HC (2014) Diverse coral communities in naturally acidified waters of a Western Pacific Reef. Geophysical Research Letters 41:499-504
Shamberger KEF, Feely RA, Sabine CL, Atkinson MJ, DeCarlo EH, Mackenzie FT, Drupp PS, Butterfield DA (2011) Calcification and organic production on a Hawaiian coral reef. Marine Chemistry 127:64-75
Shaw EC, McNeil BI (2014) Seasonal variability in carbonate chemistry and air–sea CO2 fluxes in the southern Great Barrier Reef. Marine Chemistry 158:49-58
Shaw EC, Hamylton SM, Phinn SR (2016) Incorporating benthic community changes into hydrochemical-based projections of coral reef calcium carbonate production under ocean acidification. Coral Reefs:1-12
Sheppard CRC, Davy SK, Pilling GM (2009) The biology of coral reefs. Oxford University Press
Siciliano D (2005) Latitudinal limits to coral reef accretion: testing the Darwin point hypothesis at Kure Atoll, Northwestern Hawaiian Islands, using new evidence from high resolution remote sensing and in situ data
Signorini SR, McClain CR, Dandonneau Y (1999) Mixing and phytoplankton bloom in the wake of the Marquesas Islands. Geophysical Research Letters 26:3121-3124
Silverman J, Kline D, Johnson L, Rivlin T, Schneider K, Erez J, Lazar B, Caldeira K (2012) Carbon turnover rates in the One Tree Island reef: A 40-year perspective. Journal of Geophysical Research: Biogeosciences 117
Small AM, Adey WH (2001) Reef corals, zooxanthellae and free-living algae: a microcosm study that demonstrates synergy between calcification and primary production. Ecological Engineering 16:443-457
Smith DA, Cheung KF (2002) Empirical relationships for grain size parameters of calcareous sand on Oahu, Hawaii. Journal of coastal research:82-93
Smith S, Stoddard D, Johannes R (1978) Alkalinity depletion to estimate the calcification of coral reefs in flowing waters. Coral reefs: research methods Monographs on oceanographic methodology 5:397-404
Smith SV, Kinsey DW (1978) Calcification and organic carbon metabolism as indicated by carbon dioxide. Coral reefs: research methods 5:469-484
Smith SV, Mackenzie FT (2015) The Role of CaCO3 Reactions in the Contemporary Oceanic CO2 Cycle. Aquatic Geochemistry:1-23
SOEST UoHaM (2014) Hot Dog: Cruise Summary http://hahana.soest.hawaii.edu/hot/hot-dogs/crssum.html
Solomon S, Qin D, Manning M, Chen Z, Marquis M, Averyt KB, Tignor M, Miller HL (2007) IPCC, 2007: Climate Change 2007: The Physical Science Basis. Contribution of Working Group I to the fourth assessment report of the Intergovernmental Panel on Climate Change

Sorek M, Levy O (2012) Influence of the quantity and quality of light on photosynthetic periodicity in coral endosymbiotic algae. PloS one 7:e43264

Sowa K, Watanabe T, Nakamura T, Sakai S, Sakamoto T (2013) Estimation of uncertainty for massive Porites coral skeletal density. JAMSTEC Report of Research and Development 16:31-39

Spalding HL (2012) Ecology of mesophotic macroalgae and Halimeda kanaloana meadows in the main Hawaiian Islands. [Honolulu]:[University of Hawaii at Manoa],[August 2012],

Spalding MD, Brown BE (2015) Warm-water coral reefs and climate change. Science 350:769

Stearn C, Scoffin T, Martindale W (1977) Calcium Carbonate Budget of a Fringing Reef on the West Coast of BarbadosPart I—Zonation and Productivity. Bulletin of Marine Science 27:479-510

Stein CA, Stein S (1992) A model for the global variation in oceanic depth and heat flow with lithospheric age. Nature 359:123-129

Suzuki A, Kawahata H (2002) Carbon budget of coral reef systems: an overview of observations in fringing reefs, barrier reefs and atolls in the Indo-Pacific regions. Tellus:428-444

Suzuki A, Nakamori T, Kayanne H (1995) The mechanism of production enhancement in coral reef carbonate systems: model and empirical results. Sedimentary Geology 99:259-280

Szabados M (2008) Understanding sea level change. American Congress of Surveying and Mapping (ACSM) Bulletin:10-14

Takahashi T, Sutherland SC, Sweeney C, Poisson A, Metzl N, Tilbrook B, Bates N, Wanninkhof R, Feely RA, Sabine CL (2002) Global sea–air CO< sub> 2</sub> flux based on climatological surface ocean< i> p</i> CO< sub> 2</sub>, and seasonal biological and temperature effects. Deep Sea Research Part II: Topical Studies in Oceanography 49:1601-1622

Talley LD, Sparrow MD, Chapman P, Gould J (2007) Hydrographic atlas of the World Ocean Circulation Experiment (WOCE): Volume 2: Pacific Ocean. WOCE International Project Office

Talmage SC, Gobler CJ (2009) The effects of elevated carbon dioxide concentrations on the metamorphosis, size, and survival of larval hard clams (Mercenaria mercenaria), bay scallops (Argopecten irradians), and Eastern oysters (Crassostrea virginica). Limnology and Oceanography 54:2072

Tambutté S, Ferrier-Pagès C (2013) Effect of light and feeding on coral calcification

Thompson RW, Dickson AG, Kahng SE, Winn CD (2014) Nearshore Carbonate Dissolution in the Hawaiian Archipelago. Aquatic Geochemistry

Turner RK, Subak S, Adger WN (1996) Pressures, trends, and impacts in coastal zones: interactions between socioeconomic and natural systems. Environmental management 20:159-173

Venti A, Kadko D, Andersson A, Langdon C, Bates N (2012) A multi-tracer model approach to estimate reef water residence times. Limnol Oceanogr Methods 10:1078-1095

Veron JEN (2008) Mass extinctions and ocean acidification: biological constraints on geological dilemmas. Coral Reefs 27:459-472

Wanninkhof R (1992) Relationship between wind speed and gas exchange over the ocean. Journal of Geophysical Research: Oceans (1978–2012) 97:7373-7382

Watanabe T, Fukuda I, China K, Isa Y (2003) Molecular analyses of protein components of the organic matrix in the exoskeleton of two scleractinian coral species. Comparative Biochemistry and Physiology Part B: Biochemistry and Molecular Biology 136:767-774

Wilkinson CR (1996) Global change and coral reefs: impacts on reefs, economies and human cultures. Global Change Biology 2:547-558

Williams ID, Baum JK, Heenan A, Hanson KM, Nadon MO, Brainard RE (2015) Human, oceanographic and habitat drivers of central and western Pacific coral reef fish assemblages. PloS one 10:e0120516

Wright D, Pawlowicz R, McDougall T, Feistel R, Marion G (2011) Absolute Salinity,"Density Salinity"and the Reference-Composition Salinity Scale: present and future use in the seawater standard TEOS-10. Ocean Science 7:1-26

Wunsch C, Ferrari R (2004) Vertical mixing, energy, and the general circulation of the oceans. Annu Rev Fluid Mech 36:281-314

Yamano H, Kayanne H, Chikamori M (2005) An overview of the nature and dynamics of reef islands. GLOBAL ENVIRONMENTAL RESEARCH-ENGLISH EDITION- 9:9

Yates KK, Dufore C, Smiley N, Jackson C, Halley RB (2007) Diurnal variation of oxygen and carbonate system parameters in Tampa Bay and Florida Bay. Marine Chemistry 104:110-124

Yeakel KL, Andersson AJ, Bates NR, Noyes TJ, Collins A, Garley R (2015) Shifts in coral reef biogeochemistry and resulting acidification linked to offshore productivity. Proceedings of the National Academy of Sciences:201507021

Zeebe RE, Wolf-Gladrow DA (2001) CO2 in Seawater: Equilibrium, Kinetics, Isotopes: Equilibrium, Kinetics, Isotopes. Elsevier

Zeebe RE, Ridgwell A (2011) Past changes of ocean carbonate chemistry. Ocean acidification:1-28

Zeebe RE, Zachos JC (2013) Long-term legacy of massive carbon input to the Earth system: Anthropocene versus Eocene. Philosophical Transactions of the Royal Society 371:1-17

Tables

Table 1: Summary of Main and Northwestern Hawaiian Islands visited during Hawaii Pacific University's research cruises from 2009 to 2012. SW indicates southwest transect. NE indicates northeast transect. W indicates westward transect. E indicates eastward transect. S indicates southward transect.

	2009	2010	2011	2012
Northwestern Hawaiian Islands				
Kure Atoll		SW		
Midway Atoll		SW	SW	
Pearl & Hermes Atoll	NE & SW	NE & SW	NE & SW	NE & SW
Lisianski Island			SW	SW
Laysan Island			SW	
Maro Reef	SW		SW	NE & SW
Gardner Pinnacles			SW	SW
French Frigate Shoals	SW	SW	SW	SW
Necker Island				SW
Nihoa Island		SW	SW	SW
Main Hawaiian Islands				
Kauai Island	S			
Molokai Island	W & SW		W	
Lanai Island	NE, E & SE		E	
Hawaii Island			SW	

Table 2: TA measurement precision and accuracy.

TA Measurement Precision and Accuracy							
		Average Value	Average Difference	Standard Deviation*	CRM Batch Information		
2009 NWHI	TA CRM	2210.79	0.29	5.07	42	2210.54 +/- 0.62 umol/kg	December 16, 1997
	TA Duplicates		5.44	5.07			
2009 KOK	TA CRM	2220.11	8.90	7.28	97	2211.21 +/- 1.01 umol/kg	June 26, 2009
	TA Duplicates		2.14	4.25			
2010 NWHI	TA CRM	2215.07	3.86	3.83	97	2211.21 +/- 1.01 umol/kg	June 26, 2009
	TA Duplicates		3.96	3.82			
2011 NWHI	TA CRM	2213.54	2.33	3.46	97	2211.21 +/- 1.01 umol/kg	June 26, 2009
	TA Duplicates		4.10	3.89			
2011 KOK	TA CRM	2215.15	3.94	4.87	97	2211.21 +/- 1.01 umol/kg	June 26, 2009
	TA Duplicates		4.64	3.82			
2012 NWHI	TA CRM	2215.80	4.53	4.72	97	2211.21 +/- 1.01 umol/kg	June 26, 2009
		2237.83			122	2233.32 +/- 0.90 umol/kg	May 11, 2012
	TA Duplicates		3.86	3.52			
*Short-term standard deviation displayed for duplicate measurements.							

Table 3: Compiled biogeophysical factors by NWHI that impact calcification rate.

Island	Distance from Lo'ihi Seamount (km)[A]	Mean solar radiation (Langleys/day)[B]	Mean Summertime Surface Current (m/s)[C]	Shallow area 0-30 m (km^2)[D]
Nihoa	832	381	0.13	0.74
Necker	1108	378	0.16	1028.32
FFS	1257	361	0.14	677.96
Gardner	1505	369	0.15	-
Maro	1754	365	0.13	1075.44
Laysan	1859	367	0.14	488.13
Lisianski	2079	359	0.20	1004.27
P & H	2315	347	0.13	467.27
Midway	2476	341	0.13	101.52
Kure	2571	343	0.12	83.15

[A]Distance from Lo'ihi Seamount calculated by longitude and latitude of NWHI center (http://www.soest.hawaii.edu/GG/HCV/loihi.html)
[B]Mean year-round daily solar radiation corrected for cloud cover, units: Langleys/d (Sadler et al. 1976)
[C]Mean summertime surface current factor calculated as the mean daily Hybrid Coordinate Ocean Model (HYCOM) surface current on June 15th, July 15th, August 15th, and September 15th of 2012 surrounding each NWHI
[D]Shallow area (reef habitat) is calculated from the shoreline to the 30-m isobaths (Gove et al. 2013)

Table 4: Seasonality factor calculation table.

Month	NEC_{REEF} Bates et al. 2010 (g $CaCO_3/m^2/d$)	2008 NEC Yeakel et al. 2015 (µmol/kg)	2009 NEC Yeakel et al. 2015 (µmol/kg)	2010 NEC Yeakel et al. 2015 (µmol/kg)	2011 NEC Yeakel et al. 2015 (µmol/kg)	nTA Deficit Shaw & McNeil 2014 (µmol/kg)
Jan	5	5	1.5	-5	5	18
Feb	6	7	0	-5	7	18
Mar	7	10	5	-3	3.5	21
Apr	7.5	12.5	7	1.5	10	21
May	8	16	16	5	10	21
June	6	19.5	12	12	28	37
July	9	25	15	34.5	38	37
Aug	10.75	5	38	45	42	37
Sept	2	25	40	38	42	18.75
Oct	3.5	20	36	42.5	39	18.75
Nov	4.5	18	22.5	14	47	18.75
Dec	1.5	3	16.5	4	17	18
Annual Mean	5.90	13.83	17.46	15.29	24.04	23.69
Summertime Mean	8.58	16.50	21.67	30.50	36.00	37.00
Annual Fraction of Summertime	**0.69**	**0.84**	**0.81**	**0.50**	**0.67**	**0.64**
Mean Annual Fraction of Summertime rate			**0.69**			
Mean Annual Fraction of Summertime rate (NEC Only)			**0.70**			

Table 5: Mean nTA (µmol/kg) within the 25 m isobath for all of the NWHI. Mean ΔnTA (µmol/kg) from the surface ocean mean nTA at HOT Station ALOHA. p-value of best fit line. Maximum distance of alkalinity deficit (ΔnTA) from island center calculated from the best fit line, maximum R^2 value. The general trend in nTA values was indicated when possible as increasing, decreasing, or no change moving out from the island.

	Mean nTA (µmol/kg) within 25 m isobath	Mean ΔnTA (µmol/kg) from HOT Station ALOHA	p-value of Best Fit Line	Maximum Distance (km) of ΔnTA (Best Fit Line, R^2)	Incr or decr nTA moving out from island in SW direction	n, number of measurements
Nihoa Island	2300.7	-4.3	0.033	7.0	Increase	69
Necker Island	2272.2	-32.8	<0.001	12.0	Increase	14
French Frigate Shoals	2282.8	-22.2	<0.001	23.4	Increase	96
Gardner Pinnacles	2304.9	-	-	-	-	2
Maro Reef	2279.5	-25.5	<0.001	22.8	Increase	78
Laysan Island	2298.7	-6.3	0.227	-	Increase	30
Lisianski Island	2289.7	-15.3	0.391	-	Increase	47
Pearl and Hermes Atoll	-	-	-	-	Increase	63
Midway Atoll	2301.6	-3.4	0.048	7.8	Increase	26
Kure Atoll	-	-	0.078	-	Decrease	42

Table 6: Reef Accretion Rate calculation component values compiled with error associated displayed and the propagation of error calculated for the reef accretion rate calculation.

Model Parameters		**Standard Deviation**
Total Mean Alkalinity Concentration (µmol/kg)	32	+/-4.02
Within 25 m contour (µmol/kg)	20.7	
In surface mix layer beyond 25 m contour (µmol/kg)	7	
Below surface mix layer beyond 25 m contour (µmol/kg)	3.8	
Total Seawater Volume (km^3)	115	+/-2.5 x 10^{-10}
Within 25 m contour (km^3)	19.9	
In surface mix layer beyond 25 m contour (km^3)	31.9	
Below surface mix layer beyond 25 m contour (km^3)	63.3	
Average TEOS10 Salinity Std. Seawater Density (kg/m^3)	1023.4	+/-2 x 10^{-6}
Total Alkalinity Deficit (µmol)	**8.9 x 10^{14}**	
Conversion from alkalinity to carbon	1/2	
CaCO3 molecular weight (g/mol)	100.09	
Total Calcium Carbonate Mass (kg)	**4.5 x 10^7**	
Residence Time (days)	4.8	
Surface Velocity, HYCOM (cm/s)	16.3	+/- 4.5
Island Area (km^2)	184	+/-2.5 x 10^{-5}
Net $CaCO_3$ Production Rate ($kg/m^2/yr$)	**9.6**	**+/-2.8**
Bulk Island Density (mg/mm^3)	1.4	+/-14
% Coral Island Percent $CaCO_3$	99.9	+/-0.05
Reef Accretion Rate (mm/yr)	**10.0**	**+/-2.9**
*Standard error values from literature substituted for standard deviation		

Table 7: Sensitivity analysis of reef accretion rate calculation including surface current and island density.

Input	Primary Input Value	Impact of Alternate Inputs on Reef Accretion Rate				
Average surface current (cm/s)	HYCOM monthly summertime average, 15.7 cm/s	HYCOM June monthly average, 4379 km/yr	HYCOM July monthly average, 3532 km/yr	HYCOM August monthly average, 6721 km/yr	HYCOM September monthly average, 5152 km/yr	
		-11%	-29%	+36%	+4%	
Island density (mg/mm^3)	Avg. *Porites lobata* coral core density, Grigg 1981, 1.4 mg/mm^3	Min. *Porites lobata* coral core density, Grigg 1981, 1.2 mg/mm^3	Oahu beach sand density with 0.63 packing factor, 1.71 mg/cm^3, Hardisty 1990 & Smith and Cheung 2002	Max. *Porites lobata* coral core density, Grigg 1981, 1.53 mg/mm^3	Ishigaki min. Island skeletal density, Sowa et al. 2013, 1.45 g/cm^3	Ishigaki max. Island skeletal density, Sowa et al. 2013, 1.70 g/cm^3
		+17%	-18%	-8%	-3%	-18%

Table 8: Compiled calcification rate factors by island to estimate magnitude of alkalinity deficit. The calcification rate factors focused on were solar radiation, residence time, and shallow area (reef habitat).

	Nihoa	Necker	FFS	Maro	Laysan	Lisianski	P & H	Midway	Kure
Fraction of Mean Solar Radiation[A]	1.00	0.99	0.95	0.96	0.96	0.94	0.91	0.90	0.90
Fraction of Mean Residence Time[B]	0.90	0.72	0.82	0.87	0.83	0.59	0.87	0.91	1.00
Fraction of Shallow Area (0-30 m)[C]	0.00	0.96	0.63	1.00	0.45	0.93	0.43	0.09	0.08
Biogeophysical Factor[D]	0.63	0.89	0.80	0.94	0.75	0.82	0.74	0.63	0.66
Mean nTA[E]	2302.20	2294.06	2294.86	2289.39	2301.13	2291.93	2293.44	2305.91	2308.65
St. Dev. nTA[F]	9.59	1.31	11.48	14.61	16.52	4.31	16.55	9.00	10.16

[A]Fraction of mean daily solar radiation to maximum mean value in NWHI (Sadler et al. 1976) (Grigg 1983).
[B]Fraction of mean residence time to maximum mean residence time calculated in NWHI. Mean residence time calculated as the inverse of the mean summertime surface current factor calculated as the mean daily Hybrid Coordinate Ocean Model (HYCOM) surface current on June 15th, July 15th, August 15th, and September 15th of 2012 surrounding each NWHI.
[C]Fraction of shallow area (0-30 m) to maximum shallow area reported in NWHI (Gove et al. 2013).
[D]Biogeophysical factor calculated as the mean of the fractional solar radiation, residence time, and shallow area.
[E]Mean nTA measured in the surface mix layer and within 2.5 kilometers of the 25 m isobaths at each island.
[F]Standard deviation of the mean nTA measured in the surface mix layer and within 2.5 kilometers of the 25 m isobaths at each island.

Table 9: Compiled net $CaCO_3$ production rate and reef accretion rate estimates for comparison with our study results.

Location	Latitude	Spatial Scale	Depth Range (m)	Temporal Range	Calcification Rate (kg/m^2/yr)	Reference
Hydrochemical						
Gulf of Aqaba	29°N	Fringing Reef	1.5 - 1.8	Winter & Summer	1.8	Silverman et al. 2007
Okinawa, Japan	26°N	Reef Flat	2 - 4	Summer & Fall	7.9	Ohde & van Woesik 1999
Shiraho Reef, Japan	25°N	Forereef	0 - 1	September	5.7	Suzuki et al. 1995
Shiraho Reef, Japan	24°N	Fringing Reef	0 - 5	Spring	3.7	Kayanne et al. 1995
Japan	24°N	Reef Flat	0 - 3	Summer	1.6	Nakamura & Nakamori 2009
French Frigate Shoals, Hawaii	24°N	Island Platform	0 - 35	Summer	9.6	This Study
Kaneohe Bay, Hawaii	21°N	1/2 Barrier Reef	2	Winter & Summer	5.1	Shamberger et al. 2011
Kaneohe Bay, Hawaii	21°N	Full Barrier Reef	2	Winter & Summer	9.1	Shamberger et al. 2011
Hawaii, Waimanalo Bay	21°N	Patch Reef	2.2	Year-round	6.3	Lantz et al. 2014
Marshall Islands	11°N	Reef Crest	7 - 21	Fall	1.4	Smith & Harrison 1977
Line Islands	4°N	Lagoon	0.1 - 5	Summer	1.0	Smith & Pesret 1974
Great Barrier Reef, Australia	15°S	Patch Reef	1 - 5	Summer	9.2	Gattuso et al. 1996
French Polynesia	17°S	Barrier Reef	1 - 1.7	Winter	0.9	Gattuso et al. 1993
French Polynesia	17°S	Patch Reef	0.15 - 0.45	Summer	6.8	Gattuso et al. 1996
Great Barrier Reef, Australia	18°S	Patch Reef	1.1 - 2.8	Winter & Summer	4.8	Albright et al. 2013
Hydrochemical / Census-based						
Bermuda	32.23°N	Island Platform	0 - 6	Year-round	0.091-0.741	Venti et al. 2012
Moorea Island, French Polynesia	17.50°S	Reef Flat	0 - 5	Summer	4.7	Andrefouet & Payri 2000
Census-based						
Kure Atoll, Hawaiian Islands	28.39°N	Colony	10	Summertime	0.3	Grigg 1981
Bahamas	25.41°N	Varied	0 - 10	Winter	1.6	Perry et al. 2013
Kailua Bay, Hawaii	21.41°N	Full Reef	0 - 25	Variable	1.2	Harney & Fletcher 2003
Hawaii, Hawaiian Islands	19.90°N	Colony	10	Summertime	15.0	Grigg 1981
Grand Cayman	19.30°N	Varied	0 - 10	Winter	3.0	Perry et al. 2013
St. Croix	17.78°N	Varied	10	Varied	1.2	Hubbard et al. 1990
Belize	16.66°N	Varied	0 - 10	Winter	3.0	Perry et al. 2013
West coast Barbados	13.20°N	Fringing Reef	10	Annual	15.0	Stearn et al. 1977
Bonaire	12.09°N	Varied	0 - 10	Winter	5.4	Perry et al. 2013
Panama	7.82°N	Reef Flat	<6	Annual	2.6	Eakin 1996
Torres Strait	10.21°S	Reef Flat	15 - 25	Annual	1.7	Hart & Kench 2007
One Tree Island, Australia	23.50°S	Forereef	0.8	Summer	1.7-3.6	Shaw et al. 2016
One Tree Island, Australia	23.50°S	Forereef	0.6	Summer	1.2	Shaw et al. 2015
Lady Elliot Island, Australia	24.10°S	Lagoon	1	Year-round	2.8	Shaw et al. 2016
Lady Elliot Island, Australia	24.10°S	Lagoon	1	Year-round	5.3	Shaw et al. 2012

Figures

Figure 1: Map of the NWHI indicating the location of WOCE lines 14 and 16, HOT ALOHA site, and Hawaii Pacific University's sampling points.

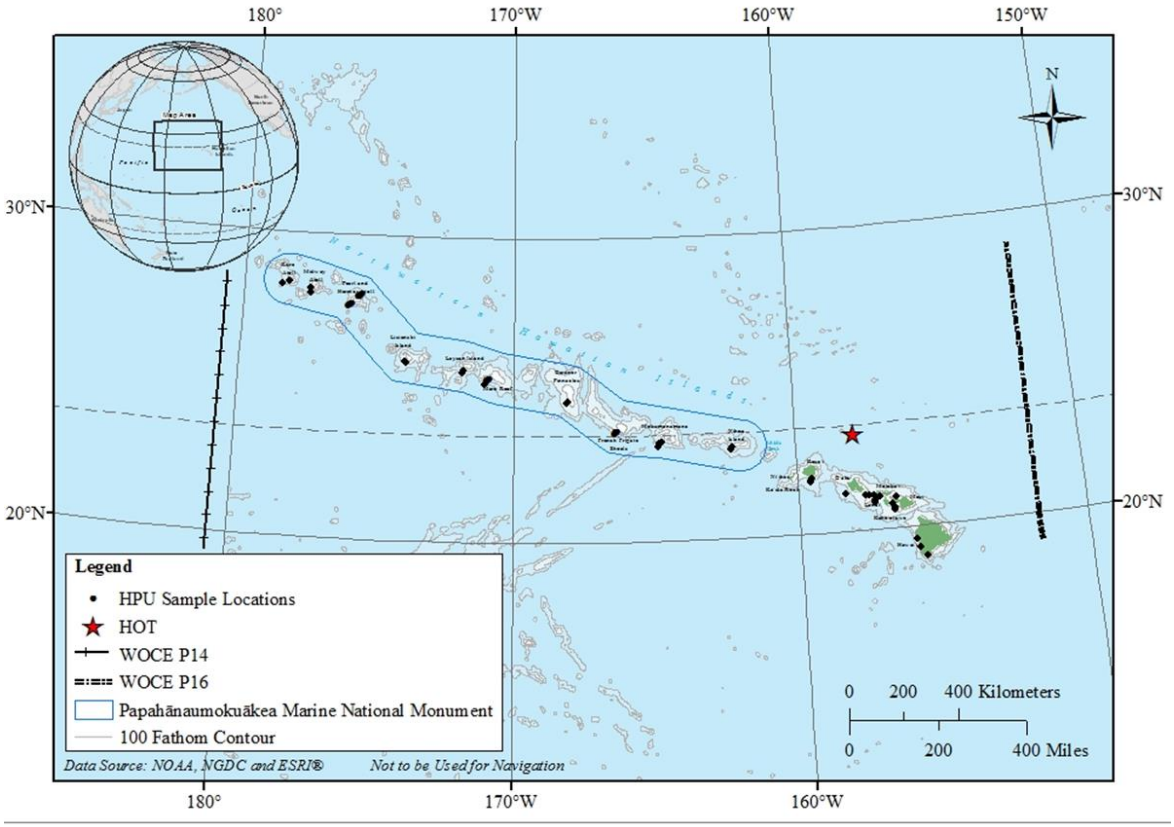

Figure 2: Illustration depicting the boundary between the surface mix layer and the subthermocline; there is very limited exchange across the boundary. A sample measured at depth A is more representative of the up current coral reef ecosystem than a sample measured at depth B.

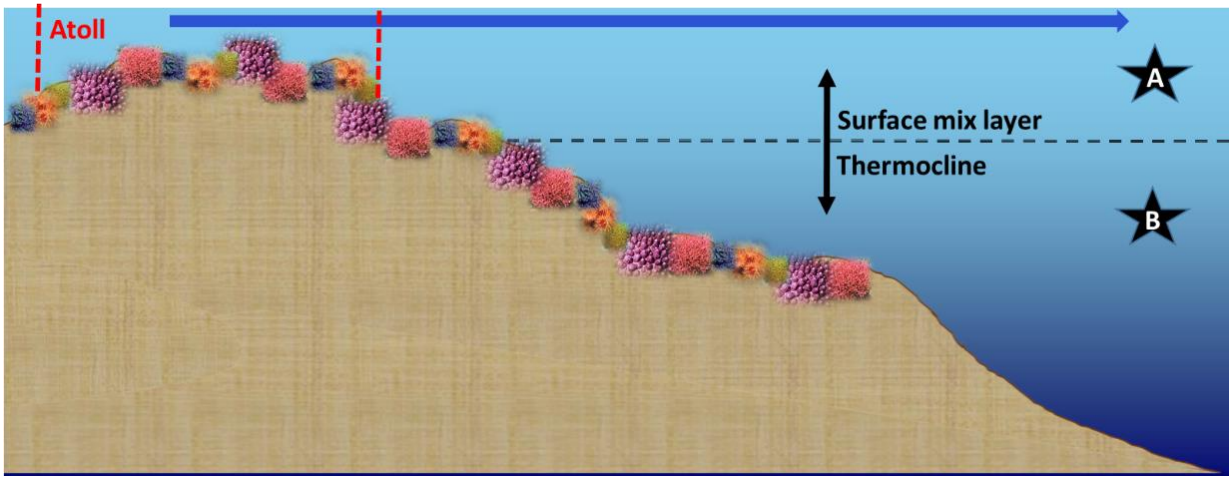

Figure 3: Illustration of 1 km^2 bins to evaluate the spatial extent of the island mass effect.

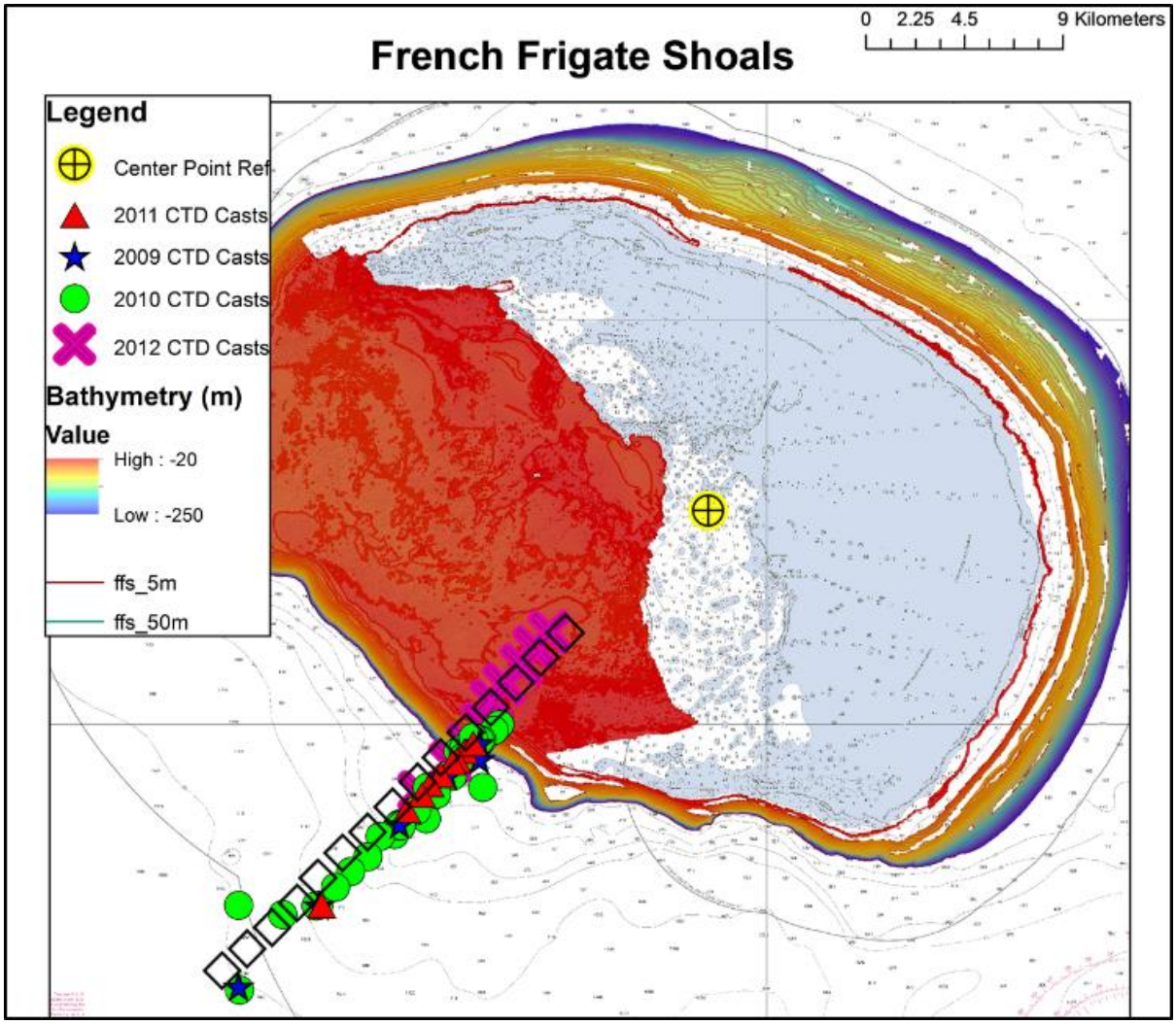

Figure 4: Illustration of 1 km^2 bins used for comparison of southwest and northeast directions from the center of Pearl and Hermes Atoll to evaluate symmetry.

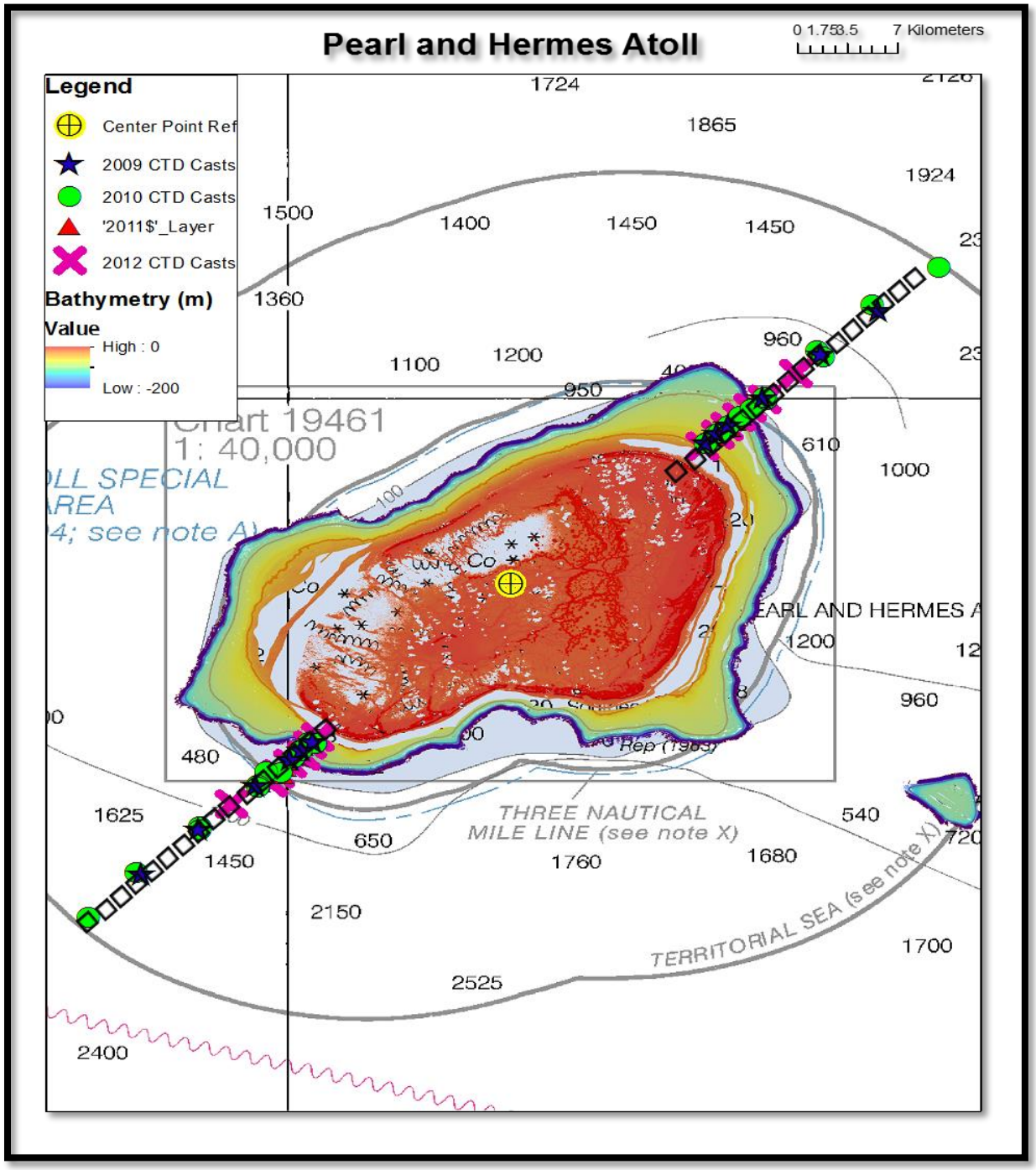

Figure 5: The graph below shows the nTA difference from the open ocean reference (HOT) with distance from the island center. The green points were in the surface mix layer and the blue points were in the subthermocline. The best fit lines are shown for each data set determined by the highest R^2 value.

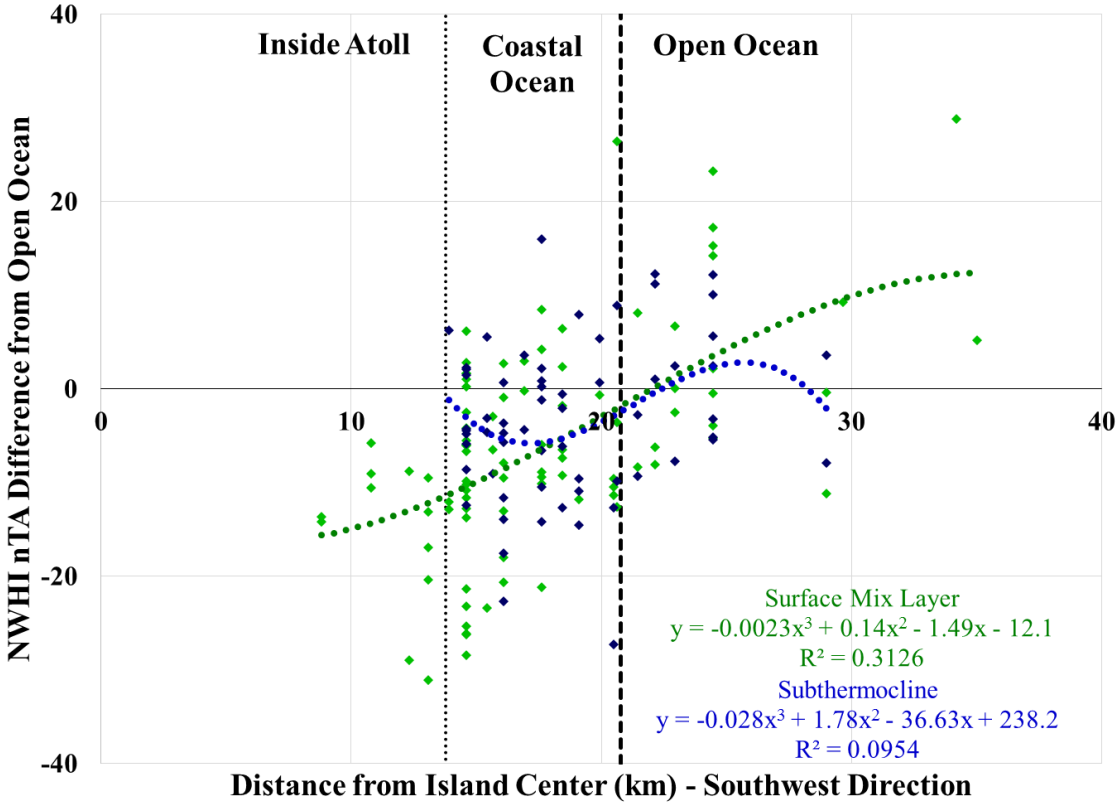

Figure 6: Illustration of nTA deficit calculation at French Frigate Shoals (FFS). Two concentric elliptical cylinders were developed around FFS, the first was at the 25 m isobath and the second was at the boundary of the impact of the island mass effect in the southwest direction.

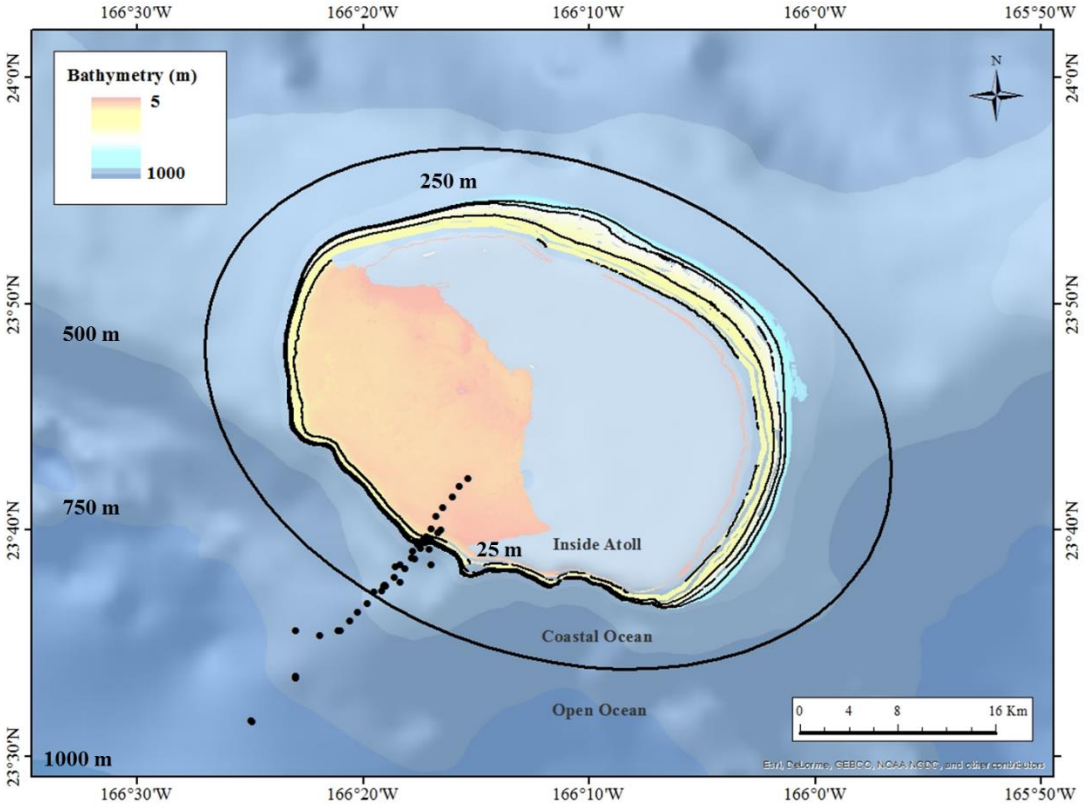

Figure 7: Calculated surface area (km^2) as a function of depth (isobath) for French Frigate Shoals (Pacific Islands Benthic Habitat Mapping Center gridded at 5 m). The 35 m isobath being utilized to delineate the accreting area at FFS is highlighted with a red line.

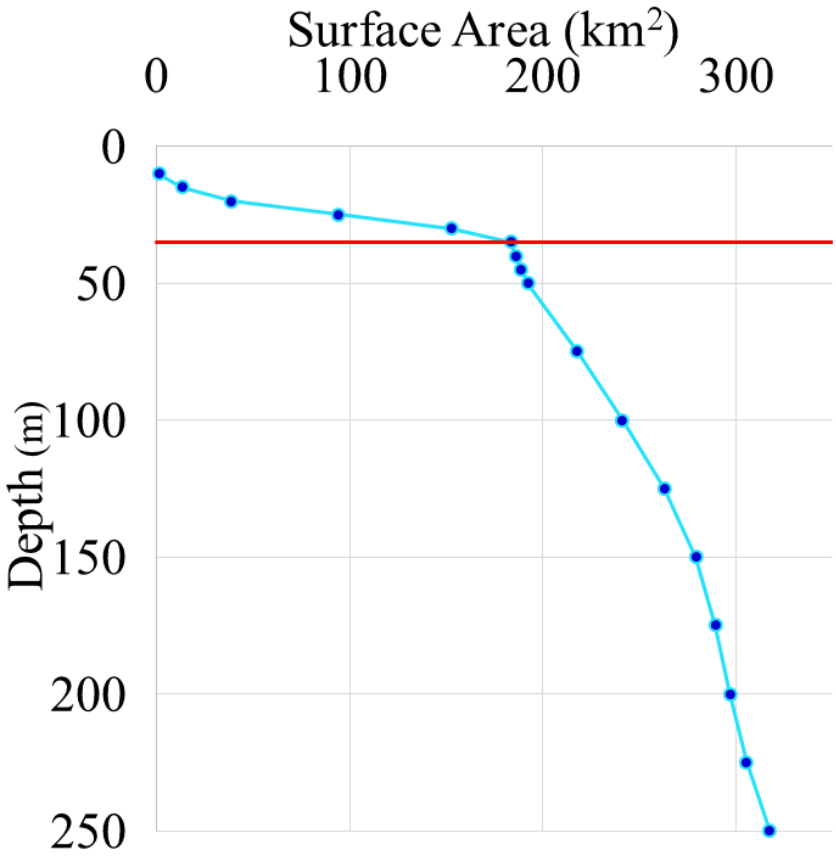

Figure 8: Northwestern Hawaiian Island (NWHI), Hawaii Ocean Time-series (HOT), and World Ocean Circulation Experiment (WOCE) lines P14 and P16 normalized total alkalinity (µmol/kg) vs pressure (dbar) and sigma theta (kg/m^3). The black circle outlines the alkalinity deficit measured in much of the NWHI not observed in the open ocean surface seawater measurements (HOT and WOCE).

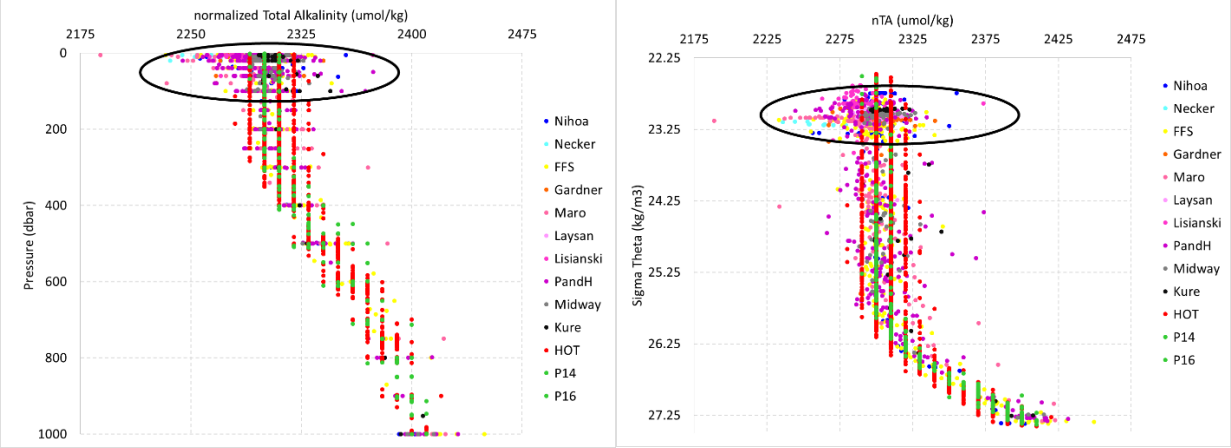

Figure 9: French Frigate Shoals (FFS) normalized total alkalinity (nTA, µmol/kg) with distance from the island center (km) moving out from FFS in the southwest direction. The data was displayed by year, but the best fit line represents data across all years, the equation and variance (R^2) was displayed on the figure. The relationship of the nTA and distance from the island center was statistically significant, $p < 0.001$.

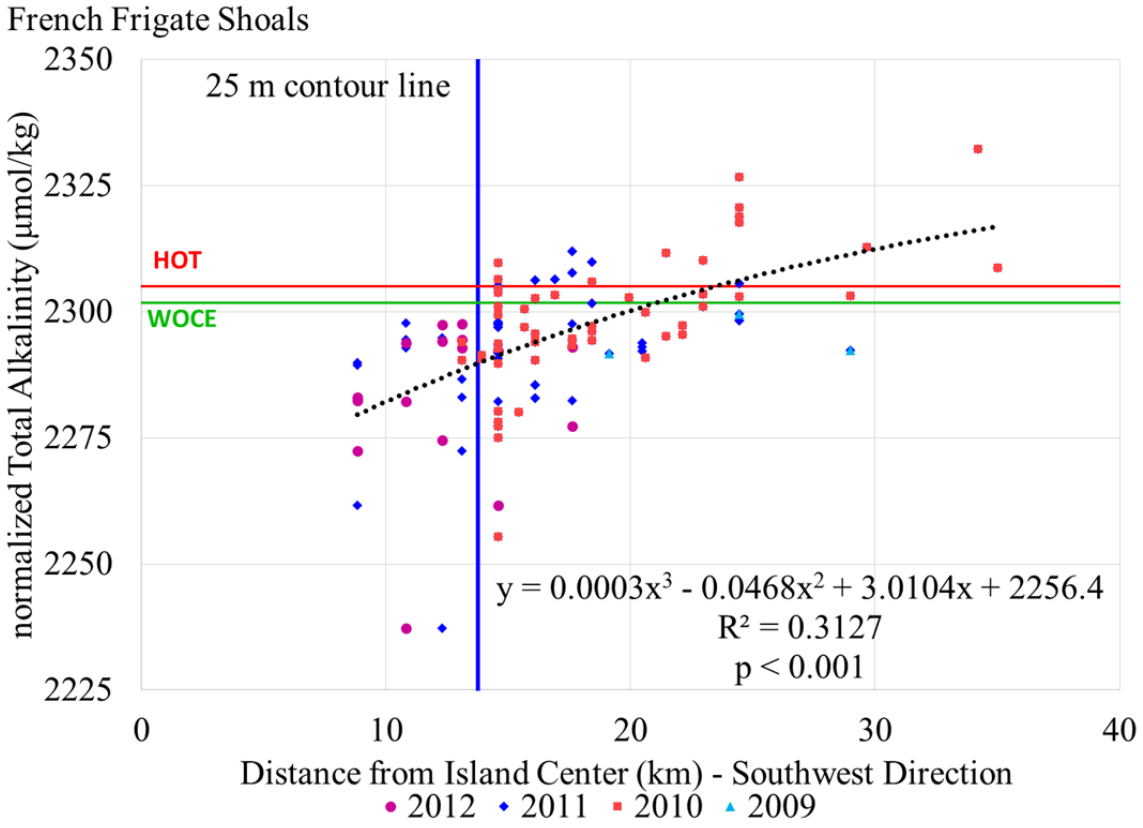

Figure 10: Boxplot of French Frigate Shoals (FFS) normalized total alkalinity (nTA, µmol/kg) with distance from the island center (km) moving out from FFS in the southwest direction aggregated by 1 km^2 distance bins. No distance bins were statistically significant using a criteria of $p<0.05$, but the distance bins that were nearly significantly different from the open ocean surface values are highlighted and indicated with a star, $p<0.10$.

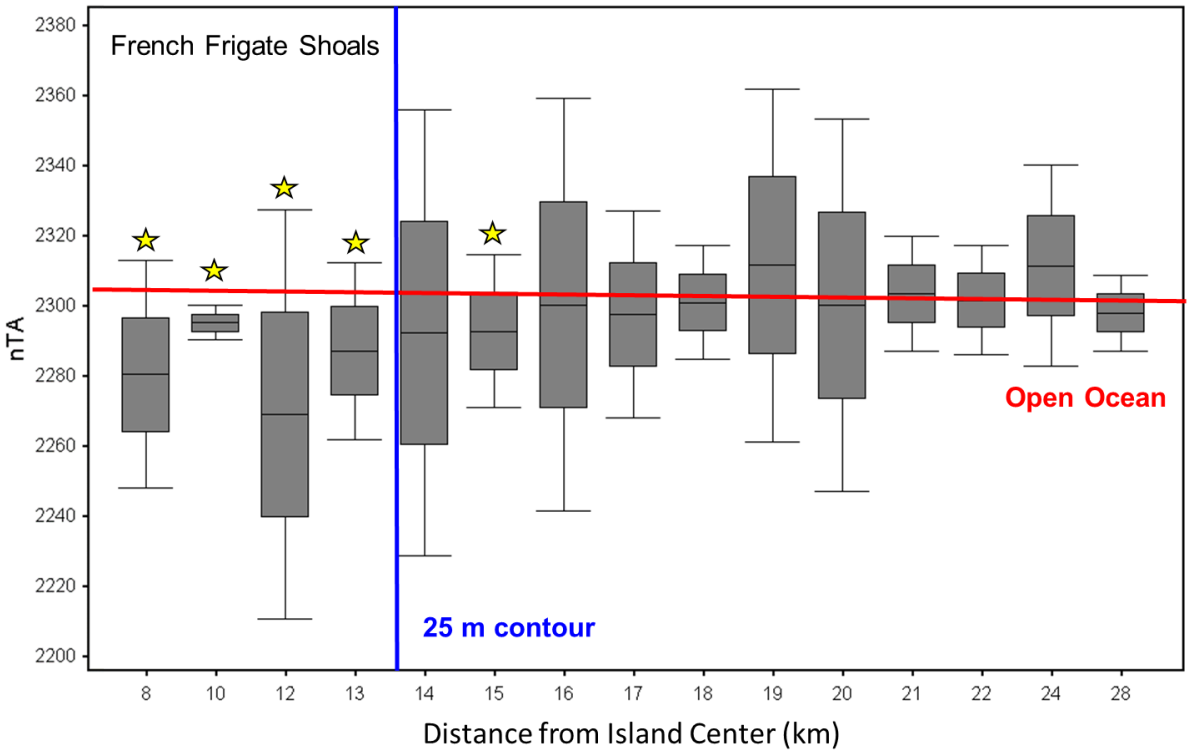

Figure 11: Northwestern Hawaiian Island (NWHI), Hawaii Ocean Time-series (HOT), and World Ocean Circulation Experiment (WOCE) lines P14 and P16 normalized total alkalinity (µmol/kg) vs sigma theta (kg/m^3). The data was binned by 0.25 kg/m^3 sigma theta ($\boldsymbol{\sigma}_\Theta$) and the average was displayed on the figure. The standard deviation was shown for all three data sets as horizontal error bars. A blue halo around the data point indicates that NWHI data point was statistically ($p<0.05$) different from the HOT or WOCE data.

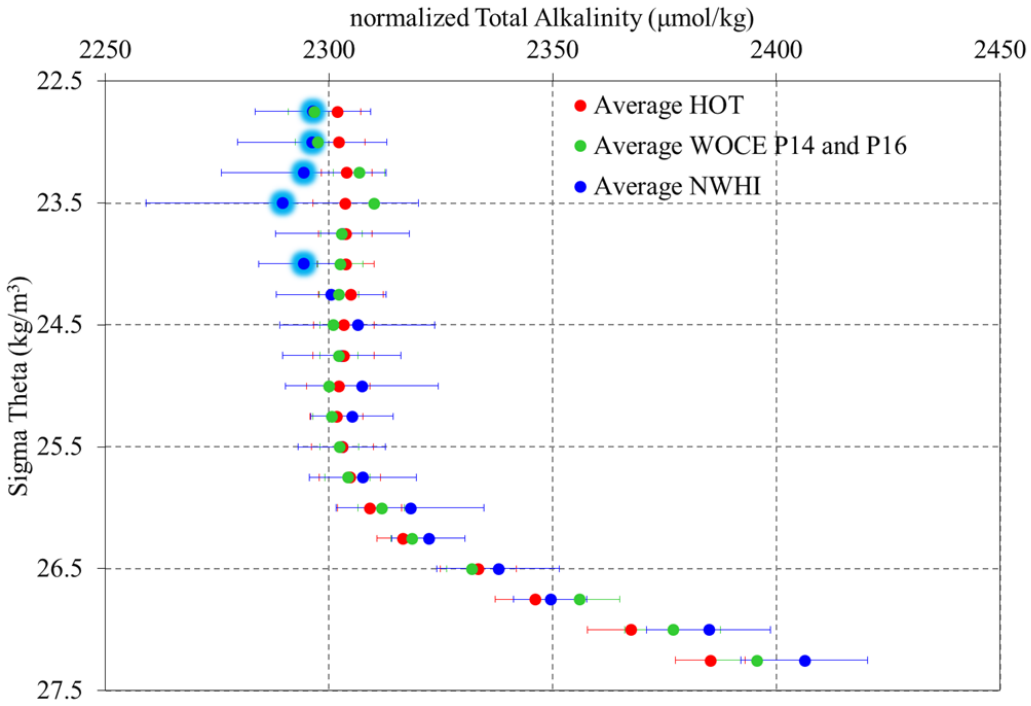

Figure 12: Northwestern Hawaiian Island pressure (dbar) vs sigma theta (kg/m^3).

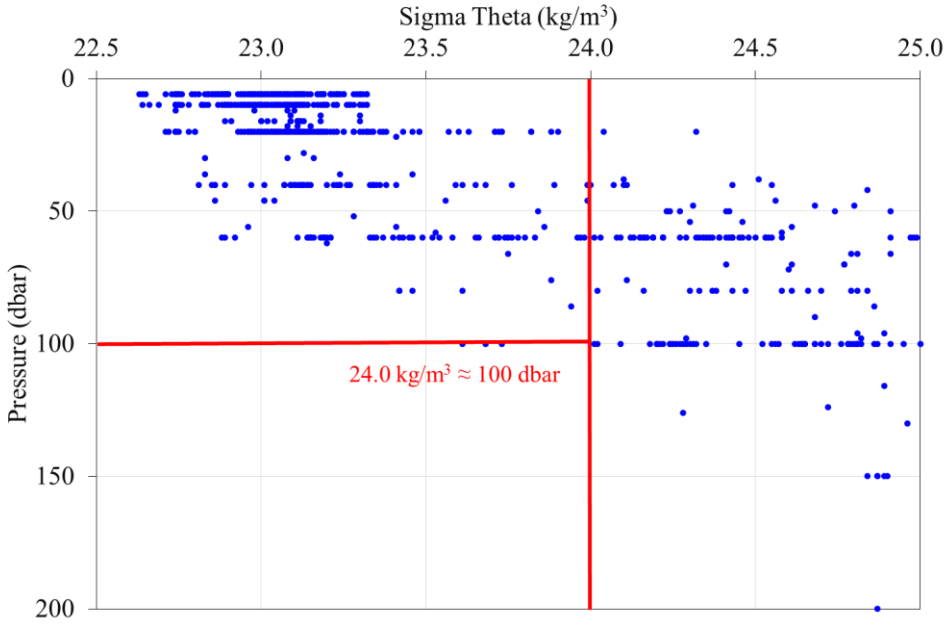

Figure 13: Pearl and Hermes Atoll (P&H) normalized total alkalinity (nTA, µmol/kg) with distance from the island center (km) moving out in the southwest or northeast direction. The best fit lines represent data across all years, the equation and variance (R^2) was displayed on the figure. The relationship of the nTA and distance from the island center in the southwest direction was not statistically significant (p = 0.42) and 20% of the variance in nTA was attributed to distance from the island. The relationship of the nTA and distance from the island center in the northeast direction was statistically significant (p = 0.02) and 20% of the variance in nTA was attributed to distance from the island.

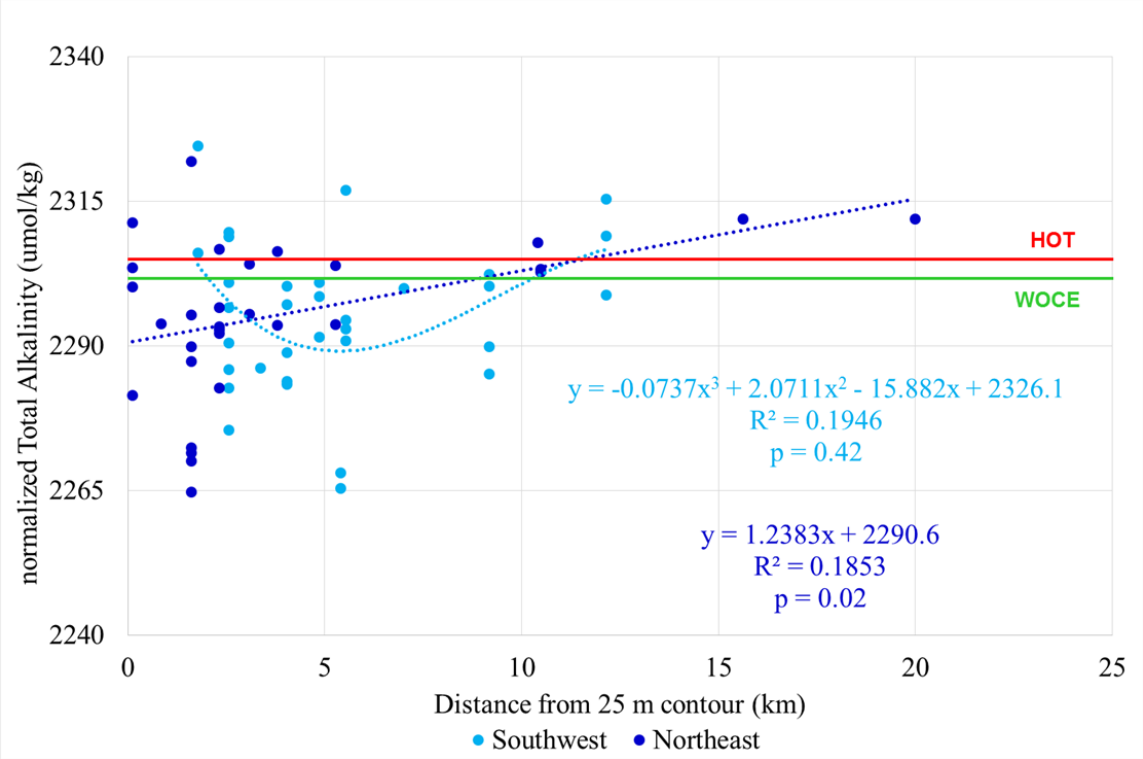

Figure 14: Normalized total alkalinity (µmol/kg) with distance from Lo'ihi Seamount (km) along the Hawaiian Archipelago. nTA measurements collected in the surface mixed layer within 2.5 km of the 25 m isobath around each island. The data are displayed by year, but the statistically significant ($p<0.01$) best fit line represents data across all years, the best fit line indicates 27% of the variance in nTA was explained by distance from Lo'ihi Seamount.

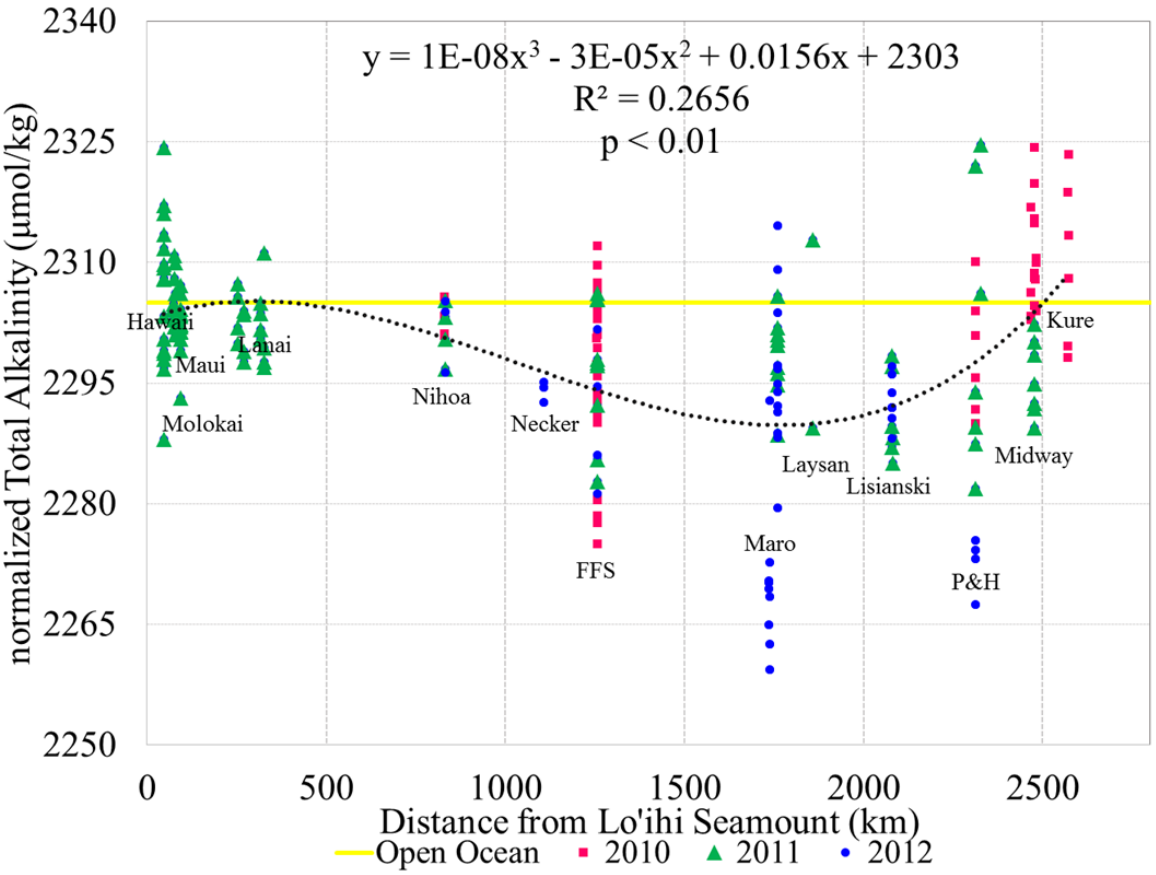

Figure 15: Boxplot of normalized total alkalinity (nTA, μmol/kg) in the surface mixed layer within 2.5 km out from the 25 m contour line southwest of the Hawaiian Islands aggregated by island. None of the islands has a mean nTA and variance that was statistically different than the rest of the islands (p = 0.499).

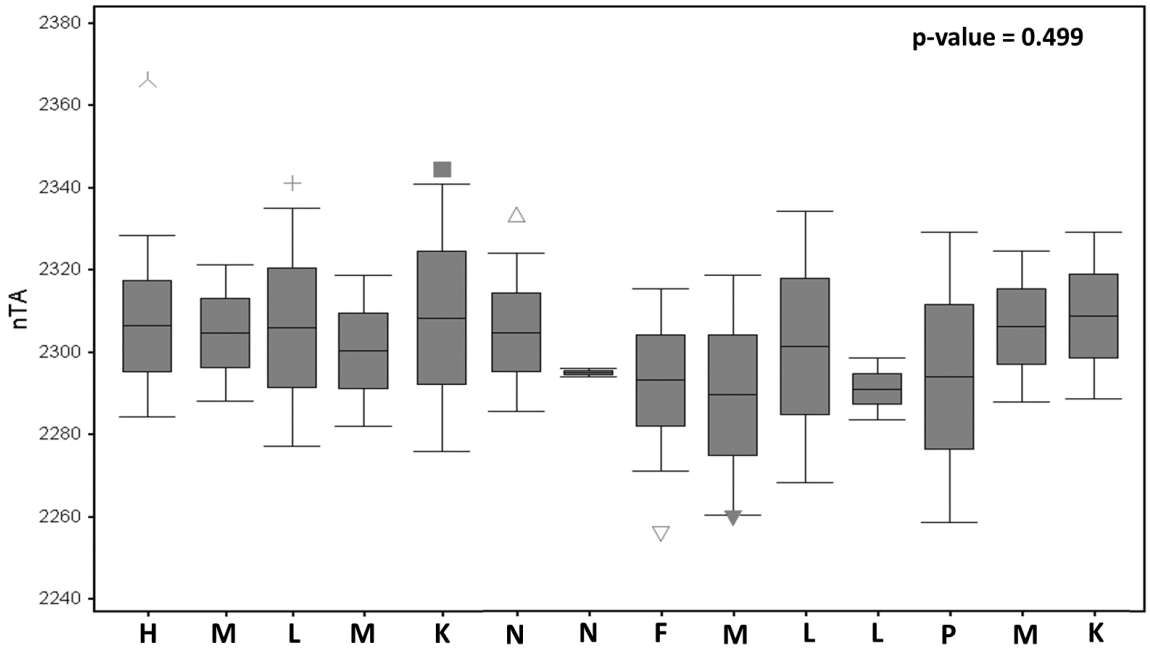

Figure 16: Correlation of the mean nTA measured in the surface mix layer and within 2.5 kilometers of the 25 m isobaths at each island and the ‘biogeophysical factor’. The relationship of the mean nTA and ‘biogeophysical factor’ was statistically significant (p = 0.003) and 75% of the variance in mean nTA was attributed to the calculated ‘biogeophysical factor’.